Noname manuscript No.
(will be inserted by the editor)

A library of Analytically Reduced Chemical schemes for a large range of CFD applications: from methane to aviation kerosene

Anne Felden · Eleonore Riber · Bénédicte Cuenot · Perrine Pepiot

the date of receipt and acceptance should be inserted later

Abstract Reacting numerical simulations today are often based on either fitted global reaction schemes, comprised of a few empirical reactions, or pre-tabulated laminar flame solutions computed with detailed chemistry. Although both methods can accurately predict global quantities such as laminar flame speed and burnt gas composition, they have significant limitations. In particular, neither are able to directly and adequately describe the complexity of pollutant chemistry. In the context of reducing harmful emissions, however, including these needed additional kinetic details in combustion simulations is becoming essential. Direct integration of detailed chemistry in accurate turbulent combustion models is not a viable option in the foreseeable future. In this context, Analytically Reduced Chemistry (ARC) represents an attractive compromise between accuracy and efficiency, and is already employed in relatively complex Direct Numerical Simulations (DNS) and Large Eddy Simulations (LES). ARCs are knowledge-based compact mechanisms retaining only the most relevant kinetic information as extracted directly, and without fitting, from detailed chemical models using specialized reduction techniques. YARC is a multi-step automated reduction tool, composed of a selected subset of very efficient reduction techniques (DRGEP, Chemical Lumping, and QSS species identification), that generates ARCs from detailed mechanisms with minimum input and knowledge from the user. This paper presents a review of recently YARC-derived ARCs for fuels ranging from methane to Jet-A aviation kerosene, along with validations in canonical test cases and, whenever possible, references of use in 3D DNS and LES.

Keywords Chemical kinetics · Reduced chemistry · Gas Turbines

1 The Analytically Reduced Chemistry (ARC) concept in numerical simulations

In the context of increasing air traffic and energy demand in the aeronautic sector, experienced over the past 30 years, the pollutants released by the combustion of aviation fuels (kerosenes, biofuels) have become a major worldwide concern. This awareness has motivated considerable actions from engine manufacturers towards the development of a new fuel-efficient generation of aeroengine combustors with low emissions. However, the simultaneous improvement of efficiency and minimization

Anne Felden
CERFACS, 42 avenue G. Coriolis, 31057 Toulouse Cedex 01, France
E-mail: felden@cerfacs.com

Eleonore Riber
CERFACS, 42 avenue G. Coriolis, 31057 Toulouse Cedex 01, France
E-mail: riber@cerfacs.com

Bénédicte Cuenot
CERFACS, 42 avenue G. Coriolis, 31057 Toulouse Cedex 01, France
E-mail: cuenot@cerfacs.com

Perrine Pepiot
Sibley School of Mechanical and Aerospace Engineering, Cornell University, New-York -14853, USA
E-mail: pp427@cornell.edu

of harmful emissions results in somewhat contradictory design trends, further complicated by constraining safety and operability specifications [50]. In particular, the intricacies of the combustion process -still not nearly enough understood today, prevent a direct control of all the parameters, prompting further research. The advent of numerical simulation tools such as Reynolds averaged Navier-Stokes (RANS), Direct Numerical Simulation (DNS), and Large Eddy Simulation (LES) [95,3,10,77], coupled to the continuously increasing available computational power, now provides a way to tackle these issues with more and more accuracy [8]. Numerical simulations of complex devices that include the description of turbulent reacting flows, are progressively becoming affordable at a design stage [8,26]. However, the capability to predict pollutant emissions relies heavily upon the fidelity of the chemistry description [100], and insights must be provided on both the dynamics of the fluid and the chemistry of the flame, as well as on their possible interactions. Unfortunately, the accurate computation of combustion chemistry -including interactions with turbulence in the context of LES, remains challenging in numerical simulations [57,10,19]. One main reason is that combustion proceeds through complex and highly non-linear processes that involve up to hundreds of different chemical compounds, with various associated time and length scales. As a result, if the progress made during the second half of the 20^{th} century regarding fundamental measurements and quantum chemistry calculations led to an improved understanding of the underlying physics, allowing the development of accurate and comprehensive detailed kinetic mechanisms, taking them into account without any simplification in large scale computations prohibitively increases the computational time and often induces stiffness in the resolved equations.

The most common simplification employed to include detailed kinetic mechanisms in CFD today is to assume that thermo-chemical evolutions in the composition/temperature space can be parameterized by a reduced set of variables. Usually, these include the mixture fraction and the progress variable. With this assumption, any thermochemical quantity of interest can be retrieved by interpolation in a database, pre-computed with detailed chemistry [60,68,27,69,75,74,2,12]. This approach drastically reduces the number of transport equations to be solved, and is thus very computationally efficient. On the downside, simulations using tabulation are very much dependent upon the type of canonical configurations chosen to build the look-up table [18,96] (premixed or diffusion archetypes, in modern tabulation techniques). If recent studies have addressed this issue [46,67,20], it remains often necessary to resort to a few additional controlling parameters, which can eventually lead to excessive memory requirements and Input/Output cost. Another major disadvantage, particularly in LES of complex real geometries, is that interactions between the flame and the flow are oversimplified. Taking into account complex phenomena such as preferential diffusion, dilution, liquid fuel, heat losses or slow pollutant chemistry then requires additional modeling efforts that can be far from trivial: additional parametrization variables are introduced, for which transport equations must be solved [17,36,63,64], resulting in additional unclosed terms. In that regard, there is also a need to formulate *a priori* assumptions about the nature of the flow.

Another classical approach consists in using globally-fitted chemical mechanisms [101,42,21, 34,84,24,44]. The idea is to split the global reaction of fuel oxidation into empirical intermediate steps. Usually, from one to four steps are considered, involving important intermediates such as CO or H_2. The reaction rate constants are expressed in an Arrhenius form, the various parameters of which are fitted against detailed chemistry results or experiments within a specified operating range, to yield good results on global flame parameters (namely, temperature and laminar flame speed). Here also, the method is CPU-efficient due to the small number of transported variables. However, the physics of the problem (i.e., the true chemical pathways) is completely lost, and only a very narrow range of operating conditions is covered. Furthermore, pollutant information is either unavailable (soot, NOx) or inaccurate (CO). A possible remedy to these drawbacks is to employ so-called "hybrid" techniques, relying upon the definition of a progress variable compatible with that of a tabulation technique so as to retrieve missing information (soot precursors, intermediate species, NO_x) from a look-up table [49,39]. However, the drawbacks associated with tabulation are retrieved.

Driven by the same necessity to reduce the high dimensionality of detailed chemistry for further investigation, physics-oriented reduction techniques have been developed [73,32,1,31]. By performing a targeted mathematical analysis of the timescales and species fluxes in a detailed reaction mechanism, the main competing chemical pathways involved in specific combustion applications can be identified, and unnecessary kinetic information can be safely discarded. The fundamental aspect of reduced mechanisms obtained by these methods, referred to below as Analytically

Reduced Chemistry or ARC, is that expressions for the evolution of all species of interest are analytically obtained, and rely directly upon the detailed chemistry model. In particular, the reaction rate constants are not modified. Of particular interest with such a chemistry description is the fact that when integrated directly in a CFD code, flame/flow interactions are not frozen, and there is no need to formulate *a priori* assumptions about the nature of the flow or the complexity of the configuration. Additionally, if the key kinetic pathways are properly identified and retained, one can reasonably expect a reduced chemical model to yield realistic species compositions even outside of its strictly demonstrated domain of validity, adding well-needed robustness to complex reactive simulations.

Two different types of reduction can be applied to a detailed reaction mechanism, to yield either a *skeletal* mechanism, where a set of unnecessary species and reactions has been discarded, or an *analytical* mechanism, where reactions are combined in order to express the evolution of a few well-chosen species through algebraic relations. Both reductions have their respective set of tools and techniques, an overview of which is provided in Table 1. The most common procedure for skeletal reduction is to first identify and eliminate *redundant* species (and associated reactions), before identifying and eliminating *redundant* reactions (terminology from [90]). Techniques pertaining to analytical reduction mostly deal with stiffness removal through an investigation of the system's timescales. Usually, it is the combination of both reductions, skeletal followed by analytical, that leads to a fully reduced mechanism, or an ARC.

Skeletal reduction	Sensitivity Analysis [91,33], Principal Component Analysis [94,32] Path Flux analysis [79,23], Jacobian Investigations [1] Graph search: DRG [54], DRGX [58], DRGASA [82], DRGEP [72] Chemical Lumping [35,71]
Analytical reduction	Quasi-Steady State approximation: via CSP pointers [30,48], via LOI [52,70], via production/consumption analysis [105], via error estimation [1], via chemical intuition [73]

Table 1 Common methods to obtain ARC. Note that the provided list of references is non-exhaustive.

The concept is not new: ARCs have been obtained in a brute force way, through sensitivity and uncertainty analysis using experience, chemical intuition, and a trial-and-error approach even long before the advent of modern computers [73,32]. In fact, the Quasi-Steady State (QSS) approximation, used in the analytical part of the reduction, dates back to the early 1920's, where it was referred to as the Bodenstein method [92]. In particular, detailed mechanisms for the oxidation of hydrogen and methane have been widely investigated [87,73] during the second half of the last century; noteworthy are the series of papers by Turanyi and co-workers on the subject [89]. The limitation in these early studies to small hydrocarbons is due to several facts [8]. First, the investigated mechanisms were all that computational capacities were able to handle at that time. More importantly, a comprehensive understanding of the underlying kinetic processes of heavier hydrocarbons is a rather recent development and still an active area of research. Finally, it has long been known that the heaviest hydrocarbon mechanisms rely strongly on lighter hydrocarbon mechanisms, from which they derive their main features. In the past decade, however, the growing need for more detailed kinetic information in relatively large and complex numerical simulations has motivated efforts towards the development of accurate ARCs for large hydrocarbons, specifically tailored for an implementation in CFD codes [51,104,13]. Typically, retaining from 10 to 30 species (depending upon the fuel) is nowadays affordable in relatively large LES [66,43,28,25,40, 83,16,22,15]. Additionally, this interest outside of the "pure chemistry" community has driven the emergence of efficient numerical tools to help perform kinetic reductions in a systematic fashion. These tools usually implement several techniques amongst the ones listed in Table 1, in so-called *multi-step* reduction strategies, in order to reach the maximum level of reduction possible.

In the present context, where ARCs are on the verge of becoming affordable at a design stage, the authors believe that it is of interest to compile recently derived LES-compliant ARCs for various hydrocarbons, in order to make them available to the community. As a first step towards achieving this goal, the present paper summarizes ARCs derived over the past 5 years with the multi-step reduction tool YARC [70]. Information about the applicability and range of validity of each derived mechanism are given, as well as references to further DNS or LES studies, whenever applicable.

Note that when deriving an ARC, the ultimate reference is the original detailed kinetic mechanism, and therefore, exhaustive comparisons between experiments and YARC-derived ARCs fall outside of the scope of this paper. All ARCs derived in this study are based upon well-accepted detailed kinetic mechanisms, and readers are referred to the original publications for their validation.

The paper is organized as follows: Section 2 briefly introduces the multi-step reduction concept, focusing specifically on the tool YARC [70]. Section 3 then presents a detailed example of an ARC derivation with YARC, for the case of ethylene-air oxidation, while Section 4 summarizes YARC-derived ARCs for various hydrocarbons ranging from methane to aviation kerosene. These reduced mechanisms together with a few other LES-compliant ARCs reported in the literature are analyzed in Section 5, and the data are employed to address CFD-specific issues such as the usual size and stiffness to be expected from such a chemistry description.

2 Multi-step reduction strategies: the YARC tool

2.1 Principle of multi-step reduction strategies

The different reduction techniques can be classified according to the level of reduction they allow to achieve, as done in Table 1. It is obvious that techniques belonging to different categories complement each other, and that one cannot hope to obtain the best possible ARC by employing only one of them. In fact, the "know-how" developed in the combustion community over the past decades reveals that to perform an efficient reduction, it is best to proceed in steps, starting with a skeletal reduction before searching for potential QSS species. This led to the design of multi-reduction strategies, where each step is enabled by borrowing from techniques belonging to each category. Note that the skeletal reduction can be comprised of several steps. To illustrate the discussion, Table 2 reports three multi-step reduction strategies reported in the literature: consistently with the previous remarks, all follow the same organization.

	Strategy I [55]	**Strategy II** : YARC [70]	**Strategy III** : KINALC [90]
STEP I Species reduction	DRG(X/ASA)	DRGEP Chemical Lumping	Jacobian investigations
STEP II Reactions reduction	DRG(X/ASA)	DRGEP	PCA
STEP III	QSS via CSP pointers	QSS via LOI	QSS via error estimation
Examples	[55,56] and more online: [53]	[72,71,39,13] and more online: [7]	[88] and more online: [89]

Table 2 Literature review of multi-step reduction strategies. See Table 1 for references to the reduction techniques.

The required inputs to such multi-step reductions consist of a detailed mechanism, a set of *targets*, and some error tolerance. Targets, in this context, stand for both the canonical problem employed for the reduction, and the quantities for the ARC to reproduce with the best accuracy. For example, if say, the ultimate goal is to investigate a sooting ethylene non-premixed jet, generating an ARC for ethylene oxidation with a good prediction of soot precursors (like acetylene for example) based on 1-D counterflow configurations is desirable.

Note that as many reduction techniques are well designed for numerical implementation, these multi-step reduction strategies are usually automated, in multi-step reduction tools. Pioneering programs were exclusively post-processors, requiring outputs from pre-existing chemistry simulation codes, and often producing results that required further adjustment to be used in chemistry or CFD solvers. This was the case of KINAL(C) [93] or CARM [9], post-processing CHEMKIN simulations [45], or the S-STEP [61] working on results from RUN-1DL [81]. More recent tools are fully coupled with chemistry solvers, and are thus able to sequentially run the canonical test cases, carry the model reduction based upon the results, perform the subsequent numerical integration of the derived set of differential equations -thus simplifying the crucial validation step, and properly format the result for further use in CFD codes. This is the case, for example, of YARC [70], employed in this work, or the tool developed recently at CORIA [37]. Obviously, designing a reduction process as systematic as possible is highly desirable in order to facilitate the derivation of reduced

mechanisms for non-experienced users. The presentation of the YARC tool is the subject of the next section.

2.2 The YARC tool

2.2.1 Presentation

The multi-step automated reduction tool YARC was developed a few years ago by one of the authors [70]. The tool consists of a series of libraries written in Pearl, implementing the DRGEP and Chemical Lumping for skeletal reduction, and the LOI for QSS selection, as summarized in Table 2 (references given in Table 1). It is fully coupled with the chemistry solver FlameMaster [76], which solves the targeted canonical cases to reproduce. The reduction can be performed on a combination of various cases, by targeting a number of important quantities such as, for example, specific species mass fractions. The canonical cases and targets employed to guide the reduction will be discussed in more depth in subsection 2.2.2.

During the reduction process, YARC generates several reduced mechanisms with increasing error level, as well as many output files containing information about each reduced mechanism. In particular, error levels pertaining to each targeted quantity can be easily monitored. The overall reduction process with YARC is illustrated on Fig. 1. Eventually, given a set of user-specified error levels on each targeted quantity, the best possible reduced mechanism is readily identified.

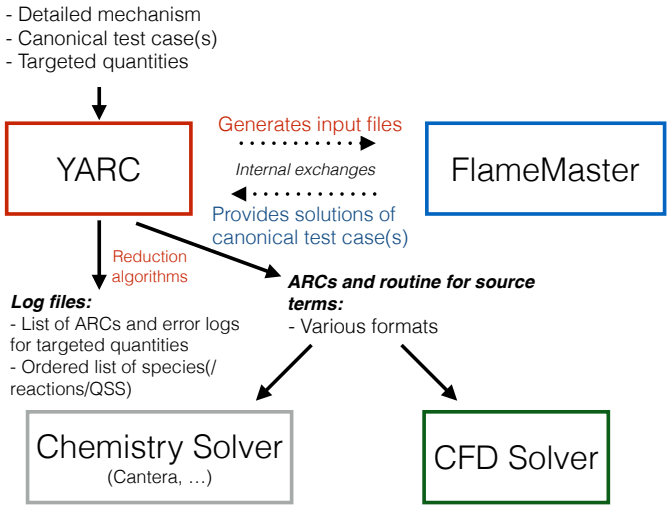

Fig. 1 Diagram of YARC

2.2.2 Targeted canonical test cases and targeted quantities

The canonical test cases employed to perform and assess the validity of the reduction of a detailed mechanism include 0-D and 1-D configurations. Belonging to the first category are constant volume or pressure batch reactors (CVR/CPR) and perfectly stirred reactors (PSR), while belonging to the second category are steady unstretched premixed laminar flames (UPF), as well as steady strained laminar diffusion flames (SDF).

When employing batch reactors, the quantity of interest is the auto-ignition timing (τ_{ig}). When using PSR, the quantity of interest is the minimum residence time, commonly accepted as a marker of extinction. In the present work, both quantities are estimated based upon the gradient of temperature. In laminar premixed or diffusion flame configurations, it is obviously of interest to recover the correct evolution of the temperature and major species (fuel, OH, CO, NO, etc.) across flame fronts. But global quantities such as the laminar flame speed (s_l), the burnt gas temperature

(T_b), the global fuel consumption ($\dot{\omega}_F^{tot}$), or the global production of major pollutants such as CO or NO ($\dot{\omega}_{CO/NO}^{tot}$) across flame fronts are also often monitored. In the present work, s_l is taken to be the inlet velocity (in UPF); while the global consumption/formation of a specific species X is estimated as:

$$\dot{\omega}_X^{tot} = \int_{c<0.98} \dot{\omega}_X dx \tag{1}$$

where x is the spatial coordinate and c is the progress variable, typically based on the evolution of CO and CO_2.

In the following (sections 3 & 4), for clarity of exposition and to ensure that a broad range of ARCs are covered, the validity of the derived ARCs is only demonstrated on a selected subset of canonical test cases, namely CVR and UPF; and for a limited range of operability consistent with respective derivation ranges. However, the range of validity (known to us) is specified for each ARC, along with references to further validation and/or applications for the interested reader. In the next section, the derivation of an ARC for ethylene-air oxidation is presented in details.

3 Example of a YARC reduction: ethylene-air oxidation

3.1 Choice of the detailed mechanism

The first step in deriving an ARC is, of course, the choice of a detailed mechanism. It is a very important step, as one cannot expect any reduced mechanism to perform better than what the detailed mechanism was designed for. Ethylene is the smallest of alkenes, and is commonly employed to investigate soot phenomena. As such, it has been widely studied from both experimental and computational points of view, and many authors have developed their own specific detailed mechanisms. Amongst them, 5 have been selected based on their availability, operating range, size, and general acceptance in the community. They are listed in Table 3.

Acronym	**Reference**	**Size**
W&F	Wang & Frenklach [97]	99 species 533 reactions
W&L	Wang *et al.* [98]	75 species 529 reactions
USCII	Wang *et al.* [99]	111 species 784 reactions
CRECK (C1-C3 high and low T mechanism)	Ranzi *et al.* [78]	107 species 2642 reactions
N&B	Narayanaswamy *et al.* [65]	158 species 1049 reactions

Table 3 Detailed mechanisms for ethylene-air oxidation

A series of experimental laminar flame speed and auto-ignition data for various initial pressures, temperatures and compositions are reported in the review by Ranzi *et al.* [78] as well as on the website of Prof. H. Wang [1]. A subset of these data was employed to evaluate and compare the global performance of each of these mechanisms. The solver Cantera [29] is used, along with a complex evaluation of the transport data.

Figure 2 (top row) reports s_l at an initial temperature of 300 K, for different initial pressures. All mechanisms perform reasonably well, with the exception of the W&F scheme, overpredicting s_l over the entire range of equivalence ratio reported. The USCII and CRECK mechanisms underpredict s_l around stoichiometry for P = 5 atm. The computations with both the W&F and CRECK mechanisms are difficult to converge, even in these simple laminar test cases. A rapid analysis of timescales (based on the diagonal of the Jacobian) did not reveal any overly small timescale for these mechanisms; however, the CRECK mechanism exhibits a lot of lumped reactions which might slow down the computation. These lumped reactions are not convenient for species reduction. In view of the auto-ignition delays shown in Fig. 2 (bottom row), the W&F mechanism is suspected to exhibit strong nonlinearities in the reaction rate expressions, although this has not been thoroughly investigated and is just the general impression after using this mechanism on simple test cases. Based on these observations, the mechanisms retained at this point are the W&L and the N&B.

[1] http://ignis.usc.edu/Mechanisms/USC-Mech%20II/USC_Mech%20II.htm

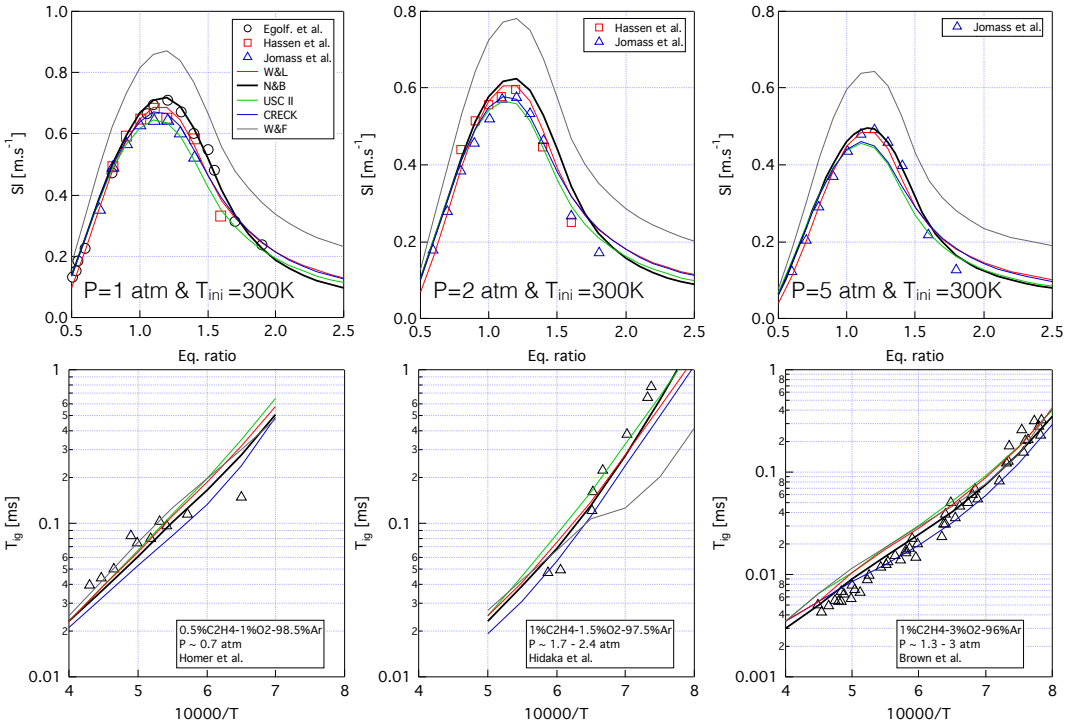

Fig. 2 Comparison of experimental laminar flame speeds (top) and auto-ignition (bottom) results with computations performed with the solver Cantera [29] and various detailed kinetic schemes (see Table 3).

The N&B is finally chosen, because it is more recent, and part of a modular comprehensive reaction mechanism still under development [2].

3.2 Choice of the targets and canonical test cases

The tool YARC is now used to perform a series of multi-step skeletal and analytical reductions of the N&B mechanism, targeting a series of operating ranges and canonical test cases, to illustrate the flexibility and efficiency of the procedure and to investigate the overall effect on the produced skeletal mechanisms. Since the detailed mechanism is of reasonable size and the targeted hydrocarbon is small, the DRGEP is only employed to remove unnecessary species. Likewise, no lumping is considered. The list and acronyms of each reduction performed is listed in Table 4. The search for QSS candidates and the derivation of a fully reduced ARC is performed in a final step, with the C_2H_2 case solely.

Case name	**Canonical test cases**	**Targeted range**	**Targeted constraints**
AI HT case	CVR	3 atm / 1300-1700 K / ϕ = 0.5-1.5	τ_{ig}, T_{eq}, CO, CO_2, OH
AI LT case	CVR	3 atm / 800-1100 K / ϕ = 0.5-1.5	τ_{ig}, T_{eq}, CO, CO_2, OH
UPF case	UPF	3 atm / 300 K / ϕ = 0.5-1.5	s_l, T_b, CO, CO_2, OH
Ref case	CVR UPF	3 atm / 1300-1700 K / ϕ = 0.5-1.5 3 atm / 300K / ϕ = 0.5-1.5	τ_{ig}, T_{eq}, CO, CO_2, OH s_l, T_b, CO, CO_2, OH
C_2H_2 case	CVR UPF	3 atm / 1300-1700 K / ϕ = 0.5-1.5 3 atm / 300K / ϕ = 0.5-1.5	τ_{ig}, T_{eq}, CO, CO_2, OH, C_2H_2 s_l, T_b, CO, CO_2, OH, C_2H_2

Table 4 List and specifications of skeletal reductions performed with YARC.

[2] http://krithikasivaram.github.io/

3.3 Effect of the targeted canonical test cases and operating range

3.3.1 CVR test cases

Two skeletal reductions exclusively on 0-D test cases have been performed, one targeting high-temperature auto-ignition (AI HT), and the other one, low-temperature autoignition (AI LT).

*Derivation of an AI HT skeletal mechanism*The detailed mechanism (N&B [65]) contains 158 species. Applying the DRGEP algorithm results in a ranked list of those species, from most important to least important, and a series of reduced mechanisms are constructed (one every 5 removed species) before being tested. The error on the prediction of the constraining targets is then calculated. For example, Fig. 3 (a) shows the error made on τ_{ig} as a function of the number of species kept in the mechanism. The error is negligible until the size of the mechanism reaches about 40 species, as evidenced by the clear jump in the error levels. Since the DRGEP only relies on the data provided by the mechanism it is applied to, in this case the detailed mechanism, it is often worthwhile to reapply it to intermediate skeletal mechanisms to take into account the eventual reorganization of kinetic pathways induced by the removal of species. This procedure is detailed next.

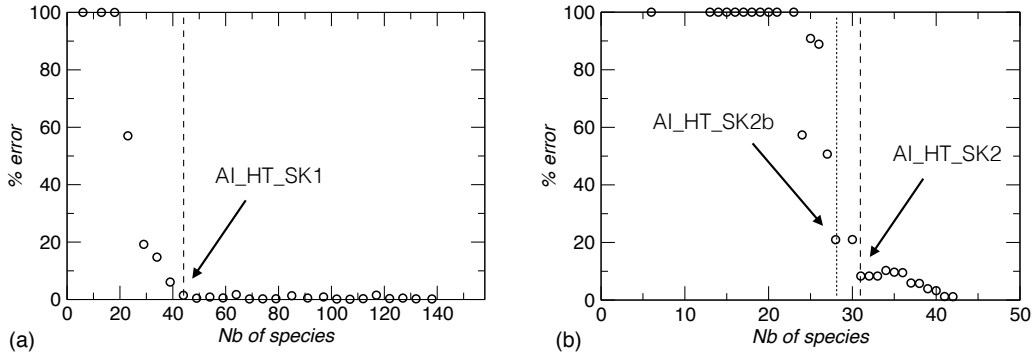

Fig. 3 Illustration of the first two DRGEP procedure: (a) on the detailed mechanism and (b) on the AI_HT_SK1 skeletal mechanism (44 species and 563 reactions).

Authorizing a maximum error of 1.5% on τ_{ig} on the first DRGEP reduction leads to the selection of a mechanism containing 44 species and 563 reactions, labelled AI_HT_SK1 in the following. If the DRGEP process is reiterated on AI_HT_SK1, a second mechanism comprised of 31 species and 379 reactions (AI_HT_SK2) is identified by the jump in the error on τ_{ig}, as shown on Fig. 3 (b). Of course, errors are now *relative* to AI_HT_SK1, and eventually, it is necessary to estimate the error relative to the original detailed mechanism. The process is reiterated once more (third DRGEP procedure), and a final mechanism of 28 species and 316 irreversible reactions (AI_HT_SK3) is obtained before the error levels become too important. A quick error estimation against the detailed mechanism on the targeted range reveals that the maximum error on τ_{ig} is $< 10\%$ for $T > 1400$ K, and peaks around 30% for $T = 1300$ K; with a maximum error for the species evolution always $< 5\%$. For the sake of simplicity, only auto-ignition delay predictions are considered in the rest of the discussion to assess the accuracy of a skeletal mechanism -verified to be the most constraining target in the present case.

As predicted, the subsequent DRGEP processes have reordered the species. For instance, keeping the order determined by the second DRGEP process to derive a 28 species mechanism directly would have resulted in a mechanism containing 28 species and 323 reactions, labelled AI_HT_SK2b, as shown in Fig. 3 (b). However, the list of species considered AI_HT_SK2b and AI_HT_SK3 differ: AI_HT_SK2b, for example, does not retain C_3H_3 nor C_3H_2O, two species contained in the AI_HT_SK3 because the third DRGEP procedure placed them at the top of the importance list. It is then interesting to compare those two 28 species mechanisms and to investigate their differences. In this case, the global performances of the AI_HT_SK2b mechanism are slightly better, since the error on τ_{ig} is consistently $< 20\%$ for $T > 1300$ K (so, in the entire derivation range). A

closer investigation reveals that this mechanism performs better in the medium/high temperature range, whereas the AI_HT_SK3 performs better in the very high temperature range, see Fig. 4: indeed, successive DRGEP procedures tend to strengthen the targeted operating range (T > 1300 K corresponds to 10000/T < 7.7).

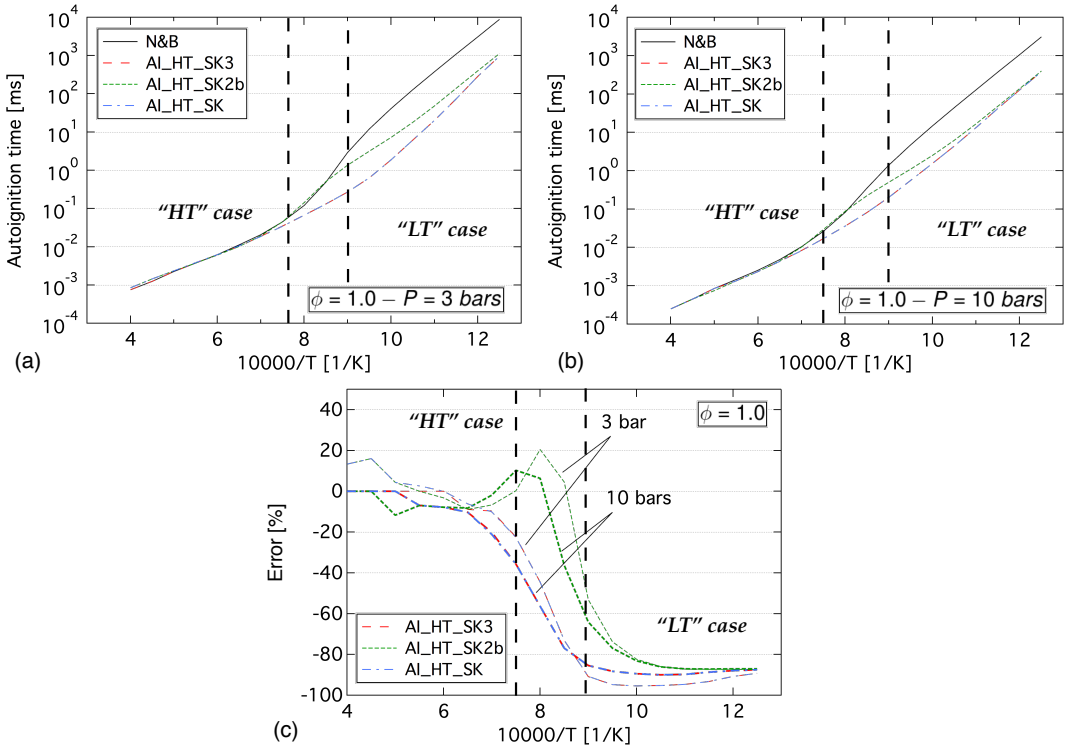

Fig. 4 Example of auto-ignition delays with the AI_HT skeletal mechanisms: (a) targeted operating range, (b) non-targeted operating pressure. Relative errors to the detailed mechanism predictions are shown in (c).

In an attempt to derive an even smaller skeletal mechanism targeting the HT range with enough accuracy (i. e. $\tau_{ig} < 10-20$ %), and since the performances of both 28 species skeletal mechanisms seem acceptable for T > 1400 K, a mechanism comprised of only those species present in both AI_HT_SK2b and AI_HT_SK3 is derived. It is comprised of 26 species and 291 reactions, and will be referred to as the AI_HT_SK. In the present case, this attempt was successful, with the AI_HT_SK exhibiting error levels similar to those of the worst 28 species mechanism in each temperature region (see Fig. 4). Note, however, that this result is by no means generalizable to any reduction procedure. Indeed, very often, the conservation of different sets of species in reduced mechanisms stems from the reorganization of pathways which could be severed entirely by such a blind way of proceeding. The validity of this approach in some cases can be attributed to reduction algorithms failures, that are to be linked to the complexity and non-linearity inherent to any chemistry process (not enough/poorly distributed samples, locally erroneous criteria, etc.) In fact, after a certain level of reduction has been attained, some trial-and-error and/or sensitivity analysis is almost always inevitable. Nonetheless, this example has demonstrated that *most* of the reduction process can be done systematically, without prior chemistry knowledge: amongst the three skeletal mechanisms derived for the prediction of HT AI in this section, the AI_HT_SK2b and AI_HT_SK3 perform extremely well in the derivation range 1400 < T < 2000 K, with errors on τ_{ig} and targeted species evolution never exceeding 20% and 5%, respectively. These skeletal mechanisms were obtained directly, with respectively 2 and 3 successive DRGEP procedures applied on successively reduced mechanisms, simply by an investigation of the YARC error logs. Note that going from 158 to 28 species represents a species reduction (so, CPU cost reduction at least) of 82%.

To finish, note that the performances of all skeletal mechanisms in predicting HT AI remain acceptable even well outside of the targeted operating range, as for example at P = 10 atm, $\phi = 1.0$ shown on Fig. 4 (b) & (c). This is the result of the reduction process being "physics-oriented" and

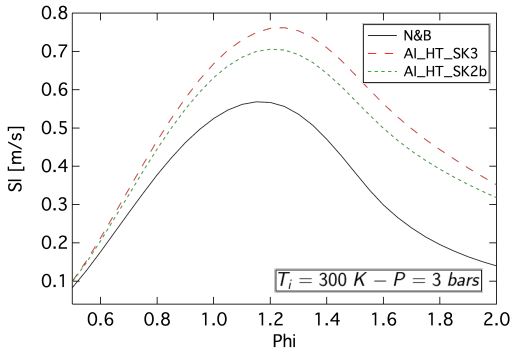

Fig. 5 Example of s_l computations for P = 3 bars and T_i = 300 K, with the AI_HT skeletal mechanisms. Comparisons are performed with the N&B detailed mechanism.

conserving the main relevant pathways, and of the kinetic process under investigation evolving continuously within the operating range, so that an ARC performance will slowly worsen outside of its derivation range. One has to be careful, however that this conclusion does not necessarily apply to other canonical test cases (in particular, when transport plays an important role). In the present case for example, global performances of the smallest skeletal mechanisms (AI_HT_SK2b, AI_HT_SK3, AI_HT_SK) on simple premixed laminar 1D test cases, such as s_l, are very poorly predicted (see Fig. 5). This is an important observation. Indeed, it is often argued in the literature that auto-ignition and extinction delays are most constraining in that they require to consider more pathways than laminar premixed or diffusion flames. However, recently, Jaouen *et al.* [38] derived a reduced mechanism for methane/vitiated-air combustion along various trajectories in the phase space, and found that the inclusion of laminar premixed flames as a target in their algorithm was necessary to retrieve the laminar flame speed accurately. This supports the findings of the present study.

*AI HT versus AI LT skeletal mechanisms*Two successive DRGEP procedure on the detailed N&B mechanism in the range targeted by the AI LT case (see Table 4) results in a skeletal mechanism comprised of 27 species and 271 reactions, labelled AI_LT_SK. A first observation is that among the species retained in the HT and LT skeletal mechanisms, only 21 are common to both. Another observation is that the performances of these mechanisms in predicting auto-ignition delay, when confronted to each other and to the detailed mechanism for the entire temperature range, are very different (see Fig. 6). This is not surprising since they have each been drastically reduced to perform very well only in their respective targeted range.

However, it is also readily observed that AI_LT_SK is more accurate over the entire temperature range: the maximum error on the prediction of τ_{ig} never exceeds 80% when it almost reaches 100% on the LT range with AI_HT_SK, see Fig. 6. If it is a well known fact that the medium/low temperature range auto-ignition is more challenging to capture in heavy hydrocarbons (typically, with a carbon content greater than 3), resulting usually in more exhaustive mechanisms containing heavy oxygenated species, the observed trends in the present study cannot be entirely attributed to this phenomenon.

*A skeletal mechanism to predict AI on the entire temperature range*Once again, some user input at this point enables to derive a skeletal mechanism valid over the entire temperature range. Note that the AI_LT_SK performances are excellent everywhere except in the very high temperature range where the AI_HT_SK results are more accurate. As previously mentioned, both skeletal mechanisms only share 21 species in common. As a result, it is attempted to include a subset of species exclusively contained in the AI_HT_SK in the AI_LT_SK in order to improve its predictive capabilities on the HT range. A path flux analysis performed on the HT range with the AI_HT_SK, directly in Cantera, reveals that the CH_2CO species -discarded in the AI_LT_SK, is part of a major pathway. The new LT skeletal mechanism considering the CH_2CO kinetics now contains 28 species and 291 reactions, and is labelled AI_LT_SK+. Its performances are good over the entire temperature range, as shown on Fig. 6.

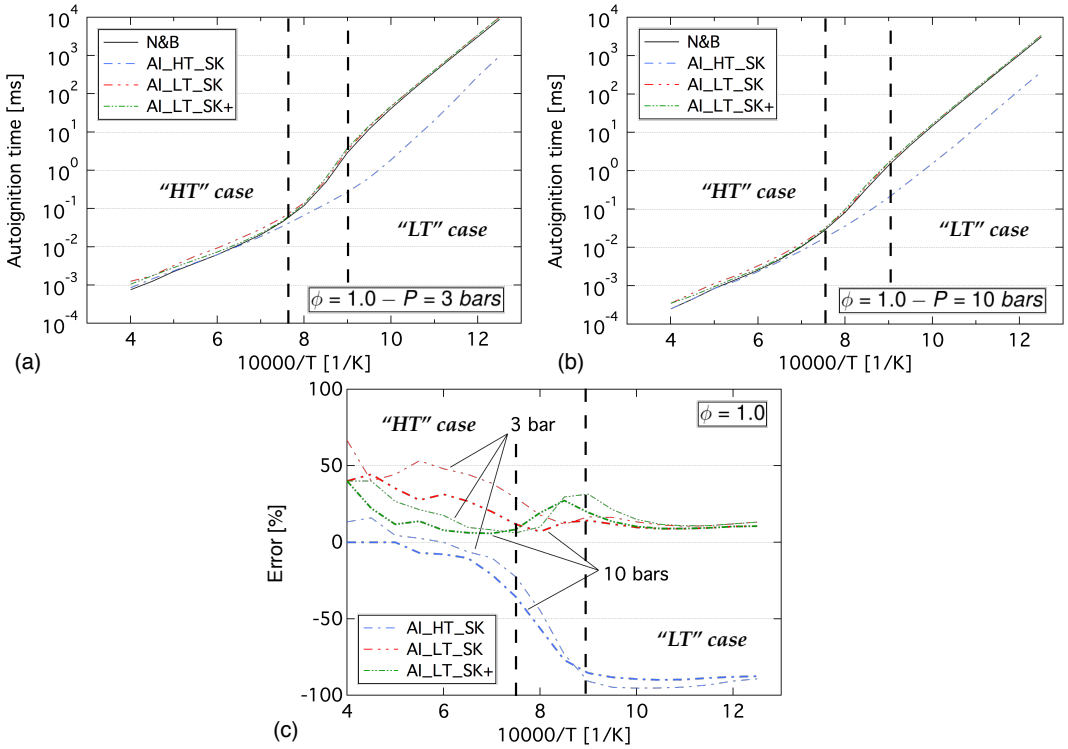

Fig. 6 Example of auto-ignition delays with the AI_HT_SK and AI_LT skeletal mechanisms: (a) targeted operating range, (b) non-targeted operating pressure. Relative errors to the detailed mechanism predictions are shown in (c).

3.3.2 UPF test cases

As previously said (Fig. 5), none of the skeletal mechanism derived on CVR test cases was able to reproduce the correct behavior in laminar 1-D premixed test cases. Thus, including UPF test cases in the reduction loop appears necessary to capture, in particular, the correct s_l. A few questions come to mind at this point, that can be summarized as follows:

- Is a reduction solely based on 1-D test cases able to retrieve auto-ignition delays ?
- Which test case is the most constraining in practice (in terms of number of species to keep) ?
- Is a reduction based on UPF able to account for strain ?
- Is a reduction based on UPF able to account for diffusion structures ?

From literature review, it is expected that the answer to the last two points is positive. To shed some light on the other interrogations, a reduction is performed on the basis of UPF solely (UPF case in Table 4).

*Derivation of a skeletal mechanism on UPF test cases*The reduction, when targeting 1-D test cases, is a bit more involved than for auto-ignition problems. For example, capturing the species spatial evolutions does not guarantee a correct laminar flame speed. Of course, this observation goes both ways. Capturing the species/temperature distribution and overall behavior in the flame zone does not guarantee that proper equilibrium levels are reached. This amounts to saying that there are more quantities to monitor, and that regular checks need to be performed during the reduction process.

A first DRGEP procedure for species elimination produces a mechanism with 34 species and 409 reactions, labelled PF_SK1, performing extremely well in the targeted range of reduction (Fig. 7). The resulting error on s_l stays below 5% in the derivation range ($0.5 < \phi < 1.5$), and is contained within 20% if the range is extended to $\phi < 2.0$. The evolution of all species of interest, characterized by peak values -usually found in the flame front, and equilibrium values, are also very well captured. CO peaks and equilibrium levels are particularly well reproduced, throughout the entire extended equivalence ratio range. The error on OH maxima is found to rapidly worsen

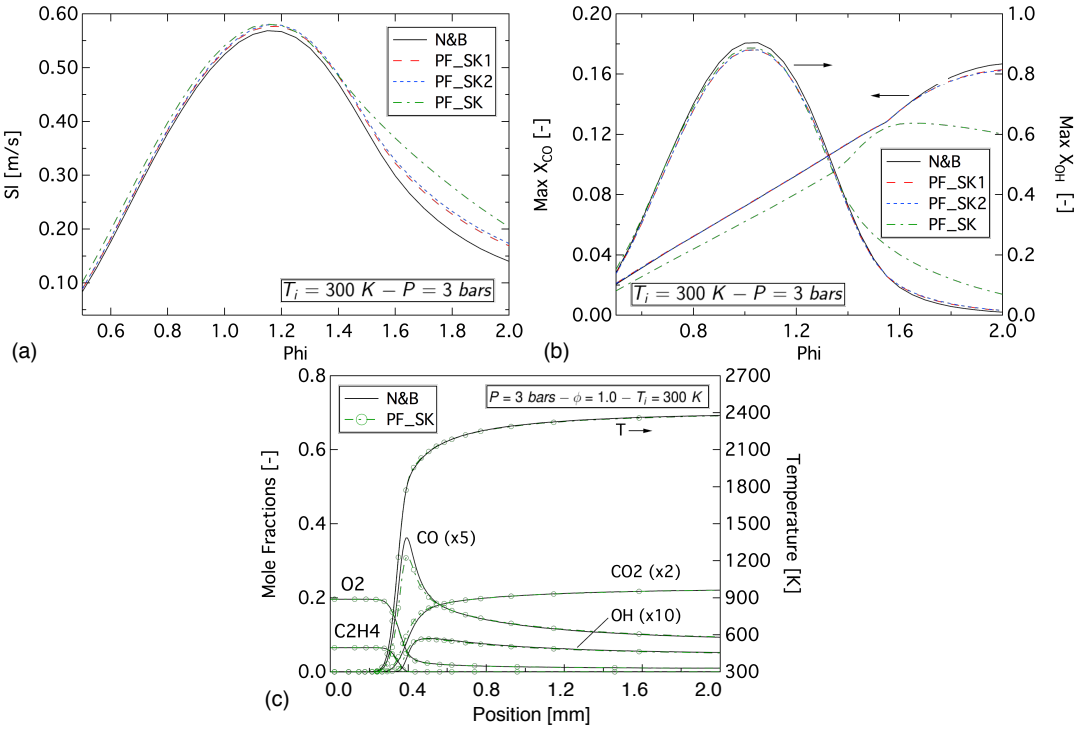

Fig. 7 Simulations of UPF for P = 3 bars and T_i = 300 K, with the UPF skeletal mechanisms: (a) laminar flame speeds, (b) maximum of CO and OH species reached in the flame fronts and (c) evolution of the major species and temperature across a stoichiometric UPF (detailed and PF_SK mechanisms).

outside of the targeted equivalence ratio range, but remains acceptable considering the very low levels found in very lean and very rich UPF (Fig. 7 (b)).

Performing these few 1D test cases reveals that the C_2H_5O species has a characteristic timescale much smaller than all other species. When deriving reduced mechanisms in view of an implementation in CFD codes, short lived species should be avoided, due to the complications that they induce in the numerical resolution (oscillations, stiffness, etc.). However, YARC places the C_2H_5O species very high in the list of species to keep. A rapid check reveals that this species remains in relatively low concentration, and only appears in a few reactions: it is thus attempted to force its elimination and all associated reactions. This does not affect the mechanism performances too much in the derivation range. A second DRGEP species reduction on this "PF_SK1 minus C_2H_5O" mechanism produces a skeletal mechanism composed of 29 species and 356 reactions (PF_SK2), predicting equally well s_l as well as major species and temperature evolutions throughout the extended equivalence ratio range (Fig. 7).

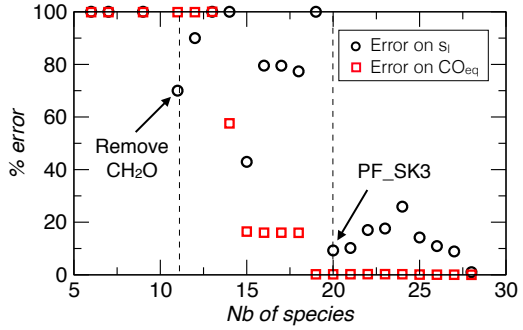

Fig. 8 Illustration of the final DRGEP procedure on the PF_SK2 skeletal mechanism (29 species and 356 reactions).

A final DRGEP procedure enables to further reduce the PF_SK2 to 20 species and 176 reactions (PF_SK3). From there, just as for the AI reductions, a certain amount of input from the user is needed to remove a few more species. In this case, a close inspection at the YARC error logs reveals several "jumps" in the error levels, see Fig. 8. These suggest the removal of CH_2O, leading to a reduction of error levels. The final skeletal mechanism, PF_SK, is composed of 19 species and 137 reactions, and its performances inside the targeted range and on the targeted quantities (reactants, CO and OH) remain acceptable (Fig. 7). Note however that predictions worsen -sometimes dramatically- outside the derivation range.

An important conclusion of the present derivation is that it was possible, at least in this case, to reduce the number of species and reactions more drastically by targeting 1-D test cases than 0-D test cases. Thus, it is expected that the UPF skeletal mechanisms will perform poorly on AI test cases. This question is addressed hereafter.

*Performances of the UPF mechanism on AI test cases*A mechanisms comparison reveals that the PF_SK1 contains the AI_LT_SK+ as a sub-mechanism. As such, the PF_SK1 is found to perform really well on the range targeted by the two AI cases. However, Fig. 9 confirms that both smaller UPF mechanisms performances (PF_SK2 and PF_SK) worsen considerably on the LT range - the mixture is even unable to auto-ignite for T $>$ 1250 K with the PF_SK mechanism. Note that the PF_SK2 and AI_LT_SK+ contain the same number of species. This analysis leads to the conclusion that, in the present case, targeting auto-ignition or premixed laminar flames lead to very different reduced mechanisms, and that one cannot hope to obtain the smallest possible mechanism accounting for both s_l and τ_{ig} without considering *both* canonical test cases. Another conclusion is that auto-ignition phenomena are more constraining, and requires the consideration of more species and pathways.

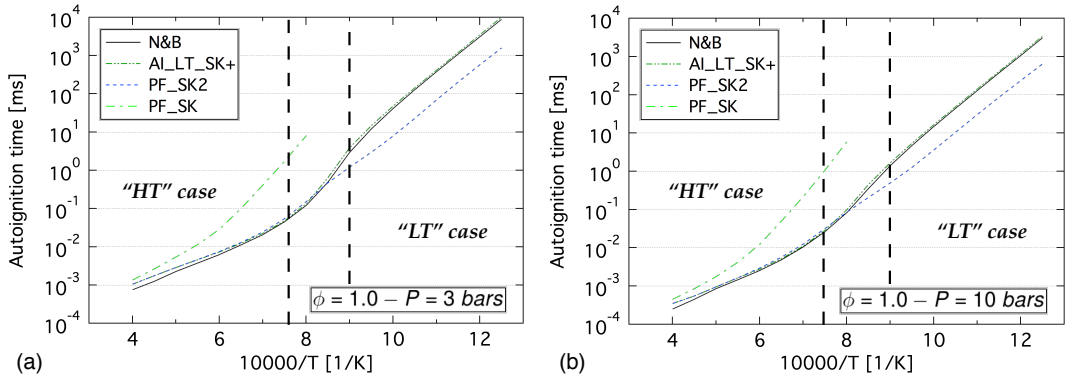

Fig. 9 Example of auto-ignition delays with the UPF mechanisms: (a) targeted operating range, (b) non-targeted operating pressure. The performance of the AI_LT_SK+ is also reported for comparison.

*Other 1-D test cases*A comparison of temperature and major species (CO, OH) evolutions across strained laminar premixed flames (same operating range than the UPF case) with various strain rates reveals that the performances of all PF mechanisms remain very good (due to a lack of space, the results are not summarized here, but details can be found elsewhere [13]). In fact, this conclusion is not that surprising, since strained premixed structures are mainly dominated by kinetic processes, and the kinetic pathways are preserved by the reduction process. Diffusion flames, on the other hand, are more controlled by the flow than the chemistry. As a consequence, diffusion structures are less accurately captured by the UPF mechanisms: profiles of temperature and major species across flame fronts exhibit the right trends, but errors increase non negligibly with increasing strain rate. The extinction strain rate, in particular, is not necessarily correctly predicted by any mechanism.

Since diffusion structures are fundamentally different from premixed structures, tests on these canonical test cases are also performed with the AI_LT_SK+ mechanism. If, globally, the performances of this mechanism are better than that of the PF_SK mechanism, the extinction strain

rate is still poorly predicted. The extinction strain rate, is thus pinpointed as being a separated phenomenon, requiring additional targets. In the literature, it is argued that targeting extinctions in constant pressure reactors rather than AI in CVR might enable to preserve the required kinetic pathways. It was not attempted in this work, but this is a possible way for improvements of the reduction process.

3.3.3 Summary

In this Section, two "standard" canonical cases and operating ranges have been considered for the derivation of reduced skeletal mechanisms, with the multi-step reduction tool YARC. Overall, it is demonstrated that the reduction process is facilitated by the automatization of the reduction procedures such as the DRGEP for species reduction, and that most of it can be carried out without any input from the user, by using the generated log files (Fig. 1). Prior knowledge from the user is only necessary in order to finalize the skeletal reduction, to remove a few more species and reactions or to merge (parts of) pre-existing kinetic schemes in a clever way.

Additionally from these remarks, a few conclusions can be drawn from these elementary tests, in order to provide a set of guidelines, tips and general "know-how" for future users of YARC and/or users of similar reduction tools:

- From a literature review, it seems undeniable that accounting for τ_{ig} on the LT range usually requires to consider more species and to preserve more pathways than accounting for τ_{ig} on the HT range, at least for "heavy" hydrocarbons (Negative Temperature Coefficient behavior, oxygenated pathways). These results seem to extend also in the present case ("small" hydrocarbon).
- Species evolutions across PF can be recovered with a mechanism reduced by targeting AI cases, but properly accounting for s_l requires to consider PF test cases in the reduction process.
- Targeting AI or PF test cases separately eventually lead to distinct reduced mechanisms, each preserving distinct kinetic pathways; and one cannot hope to derive the smallest possible ARC accounting for both s_l and τ_{ig} without considering all canonical test cases.
- From all considered test cases in this work, targeting specifically PF test cases results in the smallest set of species.
- With the exception of the extinction strain rate, the predicting capabilities of an ARC targeting PF test cases exhibit similar levels of error on the prediction of strained premixed and diffusion flames.
- None of the test cases considered in this work allow to retrieve the correct extinction strain rate.

Of course, one must bear in mind that the case employed remain fairly simple, and that the situation can get more complicated when dealing with heavier hydrocarbons, or a blend of hydrocarbons.

Following these simple guidelines, a fully-reduced ARC is derived in the next subsection, by considering both AI and PF canonical test cases. The effect of adding C_2H_2 as a target is discussed.

3.4 Derivation of an ARC for ethylene-air oxidation, with C_2H_2 as a target

3.4.1 Skeletal reduction

The exact characteristics of the skeletal reduction with C_2H_2 as a target are reported in Table 4 (C_2H_2 case). The reduction procedure is similar to what has been described in details in the first part of this Section, and is sketched in Fig. 10. Here also, some user input was required to reach the best possible skeletal mechanism (to go from 31 to 29 species).

From the analysis of the reactions kept in the 31 species and 380 mechanism, it appears that the species involved in the least reactions are CH_3O_2 and CH_3O. Both species are eventually discarded, and a mechanism comprised of 29 species and 355 reactions is obtained, referred to as the SK_NB mechanism in what follows. In this case, adding C_2H_2 as a target did not change significantly the species order when compared to a reduction performed on the Ref. case (see Table 4). The main effect is an overall importance increase of species like HCCO and CH_2CO, since they are involved in many C_2H_2 pathways. The 29 species conserved are: N_2, H, H_2, O, O_2, C, OH, HO_2, H_2O,

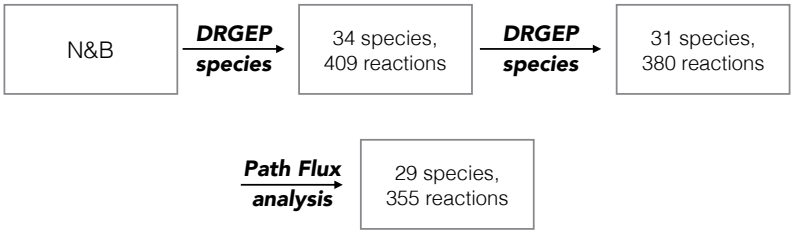

Fig. 10 Reduction process of the C_2H_2 case.

H_2O_2, CH, S-CH_2, T-CH_2, CH_3, CH_4, C_2H_2, C_2H_3, C_2H_4, C_2H_5, C_2H_6, CO, CO_2, HCO, CH_2O, HCCO, CH_2CO, CH_2CHO, CH_3CHO, C_2H_5O. Note that accounting for both CVR and UPF test cases lead to a reorganization of the pathways, such that it is now necessary to keep the C_2H_5O species to reach the best accuracy on all targets. However, note that this species could be discarded altogether, with the major effect being a worsening of performances in the AI LT range (not in the derivation range), and both a small over-prediction of s_l and C_2H_2 on rich UPF. Since, as will be discussed shortly, this species will be identified as a potential QSS candidate, it was decided to retain it.

3.4.2 Analytical reduction

The last step of the reduction process consists in identifying QSS candidates. This step is now performed, with the LOI technique implemented in YARC (Table 2), on the SK_NB. The targets remain unchanged (C_2H_2 case in Table 4). In one run, 11 species are put in QSS: C, CH, S-CH_2, T-CH_2, C_2H_3, C_2H_5, HCO, HCCO, CH_2CHO, CH_3CHO, C_2H_5O. The resulting mechanism is labelled ARC_NB in what follows. Note that the QSS assumption should degrade very little the mechanism's performances. Indeed, the error log of computations with successive ARC, resulting from incrementing the number of QSS, usually present a very distinct jump: the error goes from virtually nothing to 100%. The maximum set of QSS species is thus easily identified.

3.4.3 Validations and range of application

Global Error	*Extended range (T,P for AI, ϕ,T,P for PF)*	*Targeted range (see Table 4)*
Auto-ignition (AI)	$\phi = 0.5$: <50% (τ_{ig}) - < 2% (T-CO, OH) $\phi = 1.0$: <60% (τ_{ig}) - < 2% (T-CO, OH) $\phi = 1.5$: <70% (τ_{ig}) - < 2% (T-CO, OH)	< 50% (τ_{ig}) - < 1% (T-CO, OH)
Premixed flames (PF)	<12% (s_l) - < 10% (CO, C_2H_2) <1% (T_{ad}) - < 50% (OH)	< 2% (s_l) - < 5% (CO, OH) <1% (T_{ad}) - < 10% (C_2H_2)

Table 5 Summary of error levels of the ARC_NB mechanism on various test cases.

The performances of both the SK_NB and ARC_NB have been extensively validated against the detailed mechanism on various 0-D and 1-D test cases [15,13]. The global performances over the derivation range, as well as over an *extended* validation range are provided in Table 5. Indeed, as was already mentioned, one major advantage of ARCs is that they usually remain valid outside of their derivation range, or at the very least, their performances worsen slowly outside of targeted operating range. The *extended range* of operating conditions consist of AI with T_{ini} = 1200-3000 K and P = 1-40 bars and UPF with T_{ini} = 300-700 K and P = 1-10 bars. In fact, the extended range of operating conditions on AI test cases could be further extended to T < 1050 K: it is the region of intermediate temperatures 1100 K < T < 1300 K that is poorly accounted for with the ARC_NB. Errors refer to maximum relative errors to the detailed N&B mechanism. Examples of results are provided in Fig. 11, for both targeted and non-targeted operating points. It is stressed again that, when including CVR test cases in the derivation process, the most constraining target is τ_{ig}: as reported on Table 5, species evolutions are usually very well reproduced.

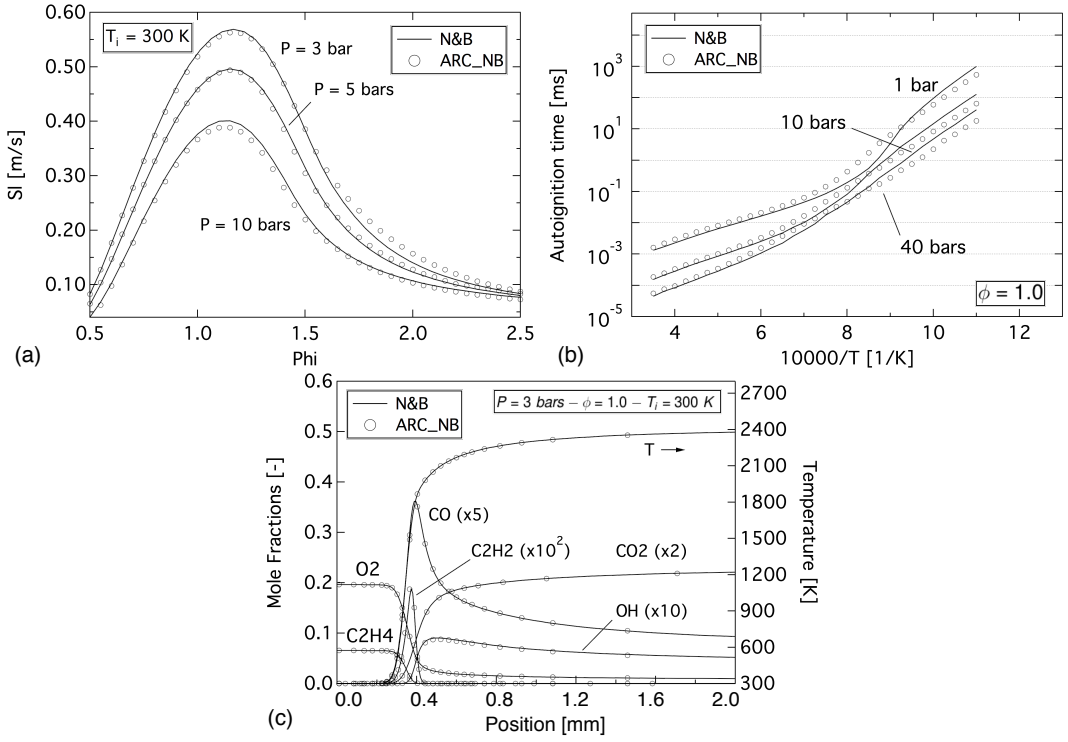

Fig. 11 Example of performances of the ARC_NB on (a) canonical UPF test cases and (b) canonical CVR test cases. (c) Evolution of the major species and temperature across a canonical UPF for P = 3 bar, T_i = 300 K and ϕ = 1.0, computed with the ARC_NB. Comparisons are performed with the N&B detailed mechanism

3.4.4 Summary

Fuel/Oxidant	Ethylene/Air
Purpose	Premixed applications, CO and soot analysis
Detailed mechanism	N&B [65]
Number of transported species/reactions/QSS	18/355/11
Transported species	H H_2 O O_2 OH H_2O HO_2 H_2O_2 CH_3 CH_4 C_2H_2 C_2H_4 C_2H_6 CO CO_2 CH_2O CH_2CO N_2
QSS species	C CH S-CH_2 T-CH_2 C_2H_3 C_2H_5 HCO HCCO CH_2CHO CH_3CHO C_2H_5O
Targeted canonical test cases	UPF: P = 3 atm T = 300 K ϕ = [0.5-1.5] AI: P = 3 atm T = [1300-1700] K ϕ = [0.5-1.5]
Targeted quantities	UPF: s_l, T_b, CO, CO_2, OH, C_2H_2 AI: τ_{ig}, T_{eq}, CO, CO_2, OH, C_2H_2
Validation range (for the targeted quantities)	UPF: P = [1-10] bars T = [300-700] K ϕ = [0.5-2.5] AI: P = [1-40] bars T = [1200-3000] K ϕ = [0.5-1.5]
Refs (more validations)	[13,15]

Table 6 YARC derived ARC for ethylene combustion

The derivation of a fully reduced ARC for ethylene-air oxidation, considering C_2H_2 as a target, was performed with the multi-step reduction tool YARC. Details regarding the derivation pro-

cess were provided. The final reduced mechanism is labelled ARC_NB, and its characteristics and performances are summarized in Table 6 and illustrated in Fig. 11.

In the next section, YARC-derived ARC mechanisms for various hydrocarbons are presented. For each of them, details regarding the derivation process are omitted. The most important information and data are summarized in tables similar to Table 6, and the validity is illustrated on representative canonical cases, as done in Fig. 11.

4 YARC reduction: from methane to kerosene

All mechanisms that are presented in this section are available in a Cantera format online [7]. Alternatively, the transported and QSS species are listed for each reduced mechanism, along with references to the detailed mechanism, so that it is possible to reconstruct each ARC easily. Note that to that end, the species names are those of the original detailed mechanisms, and the reader is referred to the reference publications for further details regarding specific species properties.

4.1 Methane

Fuel/Oxidant	Methane/Air	Methane/Air
Purpose	Premixed applications and NO analysis	Premixed applications and NO analysis
Detailed mechanism	GRI 2.11 [6]	GRI 3.0 [5]
Number of transported species/reactions/QSS	22/320/18	22/266/21
Transported species	H H_2 O O_2 OH H_2O HO_2 H_2O_2 CH_3 CH_4 C_2H_2 C_2H_4 C_2H_6 CO CO_2 CH_2O CH_3OH NO NO_2 N_2 N_2O HCN	same set
QSS species	C CH CH_2 1-CH_2 C_2H_3 C_2H_5 HCO CH_3O HCCO N NH NH_2 NNH HNO NCO HCNO HNCO HOCN	same set + CH_2OH H_2CN CN
Targeted canonical test cases	UPF: P = 1 atm T = 300 K ϕ = [0.6-1.4]	UPF: P = 1 atm T = 300 K ϕ = [0.6-1.4]
Targeted quantities	UPF: s_l, T_b, CO, NO	UPF: s_l, T_b, CO, NO
Validation range (for the targeted quantities)	UPF: P = [1-6] bars T = [300-700] K ϕ = [0.4-1.6] AI: P = [1-15] bars T = [1000-3000] K ϕ = [0.5-1.5]	UPF: P = [1-6] bars T = [300-700] K ϕ = [0.4-1.6]
Refs (more validations)	[39, 40, 83, 62]	[39]

Table 7 YARC derived ARCs for methane combustion

Two ARCs for methane-air combustion have been derived, based on either the GRIMech 2.11 [6] (ARC_GRI211) or the GRIMech 3.0 [5] (ARC_GRI30) detailed mechanisms. They were both designed to target premixed applications, and to preserve NO accuracy (global and local production); using the same canonical test cases and set of targets. Details about the derivation and validation range as well as the list of retained transported and QSS species are provided in Table 7. As in the ethylene-air case, both ARCs are shown to have a validation range that extends outside of their respective derivation range. To illustrate this, Fig. 12 (a) reports laminar flame speed values for several initial equivalence ratios and pressures. In fact, the ARC_GRI211 has also been validated on HT auto-ignition (AI) test cases, for a broad range of initial pressures (see Fig. 12 (b)).

Aside from these global quantities, the local flame structure is also very well predicted by each ARC (Fig. 13 (a) & (b)).

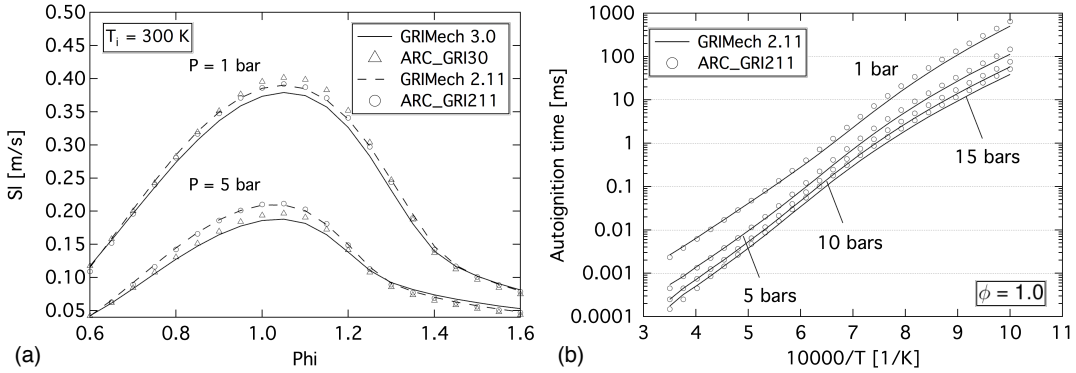

Fig. 12 (a) Example of performances of the ARC_GRI211 and ARC_GRI30 on canonical UPF test cases. (b) Example of performances of the ARC_GRI211 on canonical CVR test cases. Comparisons are performed with the relevant detailed mechanism.

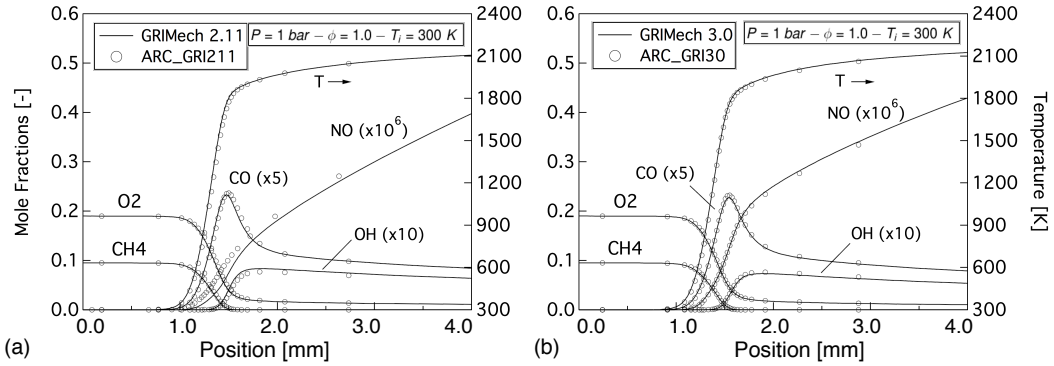

Fig. 13 Evolution of the major species and temperature across a canonical UPF for P = 1 bar, T_i = 300 K and ϕ = 1.0 with (a) the ARC_GRI211 and (b) the ARC_GRI30. Comparisons are performed with the relevant detailed mechanism.

4.2 Propane

An ARC for propane-air combustion has been derived, based on the Jerzembeck (High Temperature) version of the LLNL mechanism for *iso*-octane and *n*-heptane mixtures [41,47]. It was designed to target premixed applications (with emphasis on lean premixed applications), and to preserve CO accuracy (global and local production). Details about the derivation and validation range as well as the list of retained transported and QSS species are provided in Table 8. Figure 14 illustrates the performances of this ARC mechanism (ARC_LLNL) on various canonical test cases (targeted and non-targeted by the derivation). Note that if the mechanism is able to correctly account for τ_{ig} over a large operating range it should not be employed for high temperature auto-ignition, due to large errors on the final temperature (about 6% for T > 1600 K).

Fuel/Oxidant	Propane/Air
Purpose	Premixed applications and CO analysis
Detailed mechanism	LLNL [41,47]
Number of transported species/reactions/QSS	22/173/12
Transported species	H H_2 O O_2 OH H_2O HO_2 H_2O_2 CH_3 CH_4 C_2H_2 C_2H_4 C_2H_6 C_3H_6 C_3H_8 CO CO_2 CH_2O CH_3O_2 CH_3O_2H C_3H_5O N_2
QSS species	CH_2(S) C_2H_3 C_2H_5 C_3H_5-a i-C_3H_7 n-C_3H_7 i-$C_3H_7O_2$ n-$C_3H_7O_2$ HCO CH_3O HCCO CH_2CHO
Targeted canonical test cases	UPF: P = 1 atm T = 288 K ϕ = [0.6-1.6]
Targeted quantities	UPF: s_l, T_b, CO, CO_2
Validation range (for the targeted quantities)	UPF: P = [1-5] bars T = [288-300] K ϕ = [0.6-1.6] AI: P = [1-20] bars T = [1500-3000] K ϕ = 1.0
Refs (more validations)	[80]

Table 8 YARC derived ARC for propane combustion

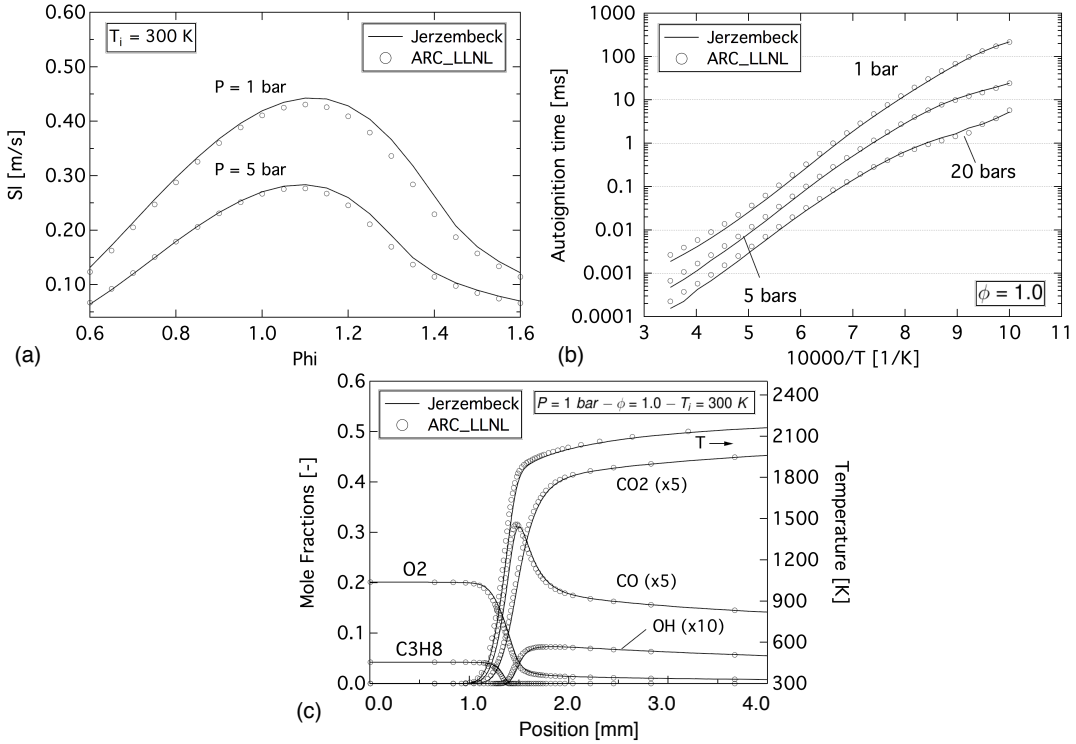

Fig. 14 Example of performances of the ARC_LLNL on (a) canonical UPF test cases and (b) canonical CVR test cases. (c) Evolution of the major species and temperature across a canonical UPF for P = 1 bar, T_i = 300 K and ϕ = 1.0, with the ARC_LLNL. Comparisons are performed with the relevant detailed mechanism [41].

4.3 Heptane

An ARC for heptane-air combustion has been derived, based on the Jerzembeck (High Temperature) version of the LLNL mechanism for *iso*-octane and *n*-heptane mixtures [41,47]. It was designed to target premixed applications, and to preserve CO/CO_2 equilibrium. Details about the derivation and validation range as well as the list of retained transported and QSS species are provided in Table 9. Figure 15 illustrates the performances of this ARC mechanism (ARC_LLNL_C7H16) on targeted canonical test cases.

Fuel/Oxidant	Heptane/Air
Purpose	Premixed applications
Detailed mechanism	LLNL [41,47]
Number of transported species/reactions/QSS	25/210/27
Transported species	H H_2 O O_2 OH H_2O HO_2 H_2O_2 CH_3 CH_4 C_2H_2 C_2H_4 C_2H_6 C_3H_4-a C_3H_6 C_4H_6 C_4H_8-1 n-C_7H_{16} CO CO_2 CH_2O HOCHO CH_3OH CH_2CO N_2
QSS species	CH CH_2(S) CH_2 C_2H_3 C_2H_5 C_3H_2 C_3H_3 C_3H_5-a n-C_3H_7 C_4H_7 p-C_4H_9 C_5H_9 C_5H_{10}-1 C_5H_{11}-1 C_6H_{12}-1 C_7H_{15}-2 HCO CH_3O CH_3O_2 CH_3O_2H HCCO CH_2CHO CH_3CO C_2H_5O $C_2H_5O_2$ n-$C_3H_7O_2$ p-$C_4H_9O_2$
Targeted canonical test cases	UPF: P = 1 atm T = 298 K ϕ = [0.6-1.6]
Targeted quantities	UPF: s_l, T_b
Validation range (for the targeted quantities)	UPF: P = [1-5] bars T = 300 K ϕ = [0.5-2.0]

Table 9 YARC derived ARCs for heptane combustion

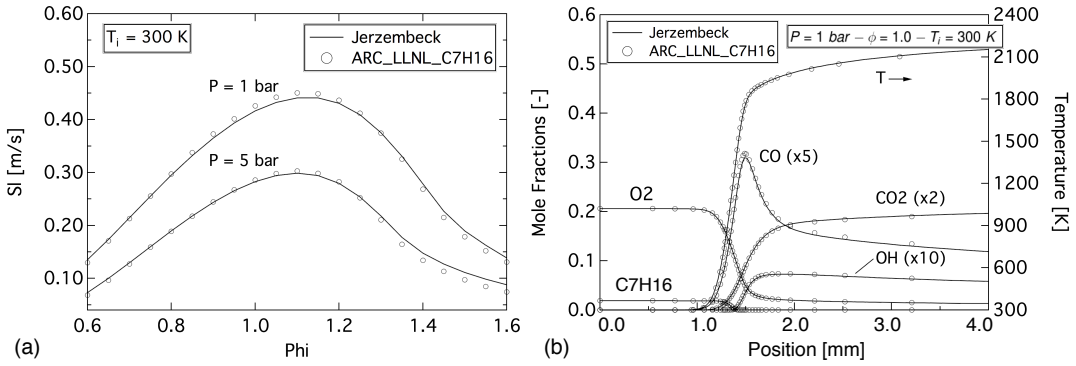

Fig. 15 Example of performances of the ARC_LLNL_C7H16 on canonical UPF test cases: (a) laminar flame speed and (b) evolution of the major species and temperature across a canonical UPF for P = 1 bar, T_i = 300 K and ϕ = 1.0. Comparisons are performed with the relevant detailed mechanism [41,47].

4.4 *n*-dodecane

Two ARCs for *n*-dodecane-air combustion have been derived based on the JetSurF 1.0-l [85], a simplified version of JetSurF 1.0 [86]. The JetSurF 1.0-l features a lumped model for *n*-alkane cracking, and the detailed USC Mech II [99] for the pyrolysis and oxidation of C1-C4 hydrocarbons. Both were designed to target premixed applications at high pressure and temperature, representative of realistic operating conditions in high overall pressure ratio engines [4]. The ARC_JetSurf_NOx was

specifically derived to preserve NO accuracy (global and local production), while the ARC_JetSurf was derived to preserve accuracy of the major soot precursor, namely, acetylene (C_2H_2), and to extend to smaller operating temperatures. Details about the derivation and validation range as well as the list of retained transported and QSS species in each ARC are provided in Table 10. Figure 16 illustrates the performances of the ARCs in various canonical test cases, targeted and non-targeted by the derivation. The ARC_JetSurf_NOx is able to correctly account for auto-ignition over a large operating range, while the validity range of the ARC_JetSurf extends to atmospheric conditions.

Fuel/Oxidant	*n*-dodecane/Air	*n*-dodecane/Air
Purpose	Partially premixed applications NO and CO analysis	Partially premixed applications CO and soot analysis
Detailed mechanism	JetSurF 1.0 [86,85]	JetSurF 1.0 [86,85]
Number of transported species/reactions/QSS	27/452/20	25/373/27
Transported species	H H_2 O O_2 OH H_2O HO_2 CH_3 CH_4 C_2H_2 C_2H_4 C_2H_6 C_3H_6 C_4H_6 C_5H_{10} C_6H_{12} n-$C_{12}H_{26}$ C_4H_81 CO CO_2 CH_2O CH_2CO NO NO_2 N_2 N_2O HCN	H H_2 O O_2 OH H_2O HO_2 H_2O_2 CH_3 CH_4 C_2H_2 C_2H_4 C_2H_6 C_3H_6 C_4H_6 C_4H_8-1 C_5H_{10} C_6H_6 C_6H_{12} n-$C_{12}H_{26}$ CO CO_2 CH_2O CH_2CO N_2
QSS species	H_2O_2 CH CH_2 CH_2* C_2H C_2H_3 C_2H_5 aC_3H_5 nC_3H_7 C_4H_7 HCO CH_3O HCCO CH_2CHO N NH NH_2 HNO NCO HNCO	CH CH_2 CH_2* C_2H H_2CC C_2H_3 C_2H_5 C_3H_3 pC_3H_4 aC_3H_5 CH_3CHCH nC_3H_7 C_4H_2 C_4H_4 iC_4H_5 C_4H_5-2 C_4H_7 o-C_6H_4 C_6H_5 $C_6H_5CH_3$ C_2O HCO CH_3O HCCO CH_2CHO H_2C_4O C_6H_5CO
Targeted canonical test cases	UPF: P = 10 bars T = 700 K ϕ = [0.6-1.4]	UPF: P = 9 bars T = [400-700] K ϕ = [0.6-1.4]
Targeted quantities	UPF: s_l, T_b, CO, NO	UPF: s_l, T_b, CO, C_2H_2
Validation range (for the targeted quantities)	UPF: P = [5-15] bars T = [700-900] K ϕ = [0.5-2.0] AI: P = [10-40] bars T = [1100-2900] K ϕ = [0.5-1.5]	UPF: P = [1-10] bars T = [300-700] K ϕ = [0.5-2.0]
Refs (more validations)	[39]	

Table 10 YARC derived ARCs for *n*-dodecane combustion

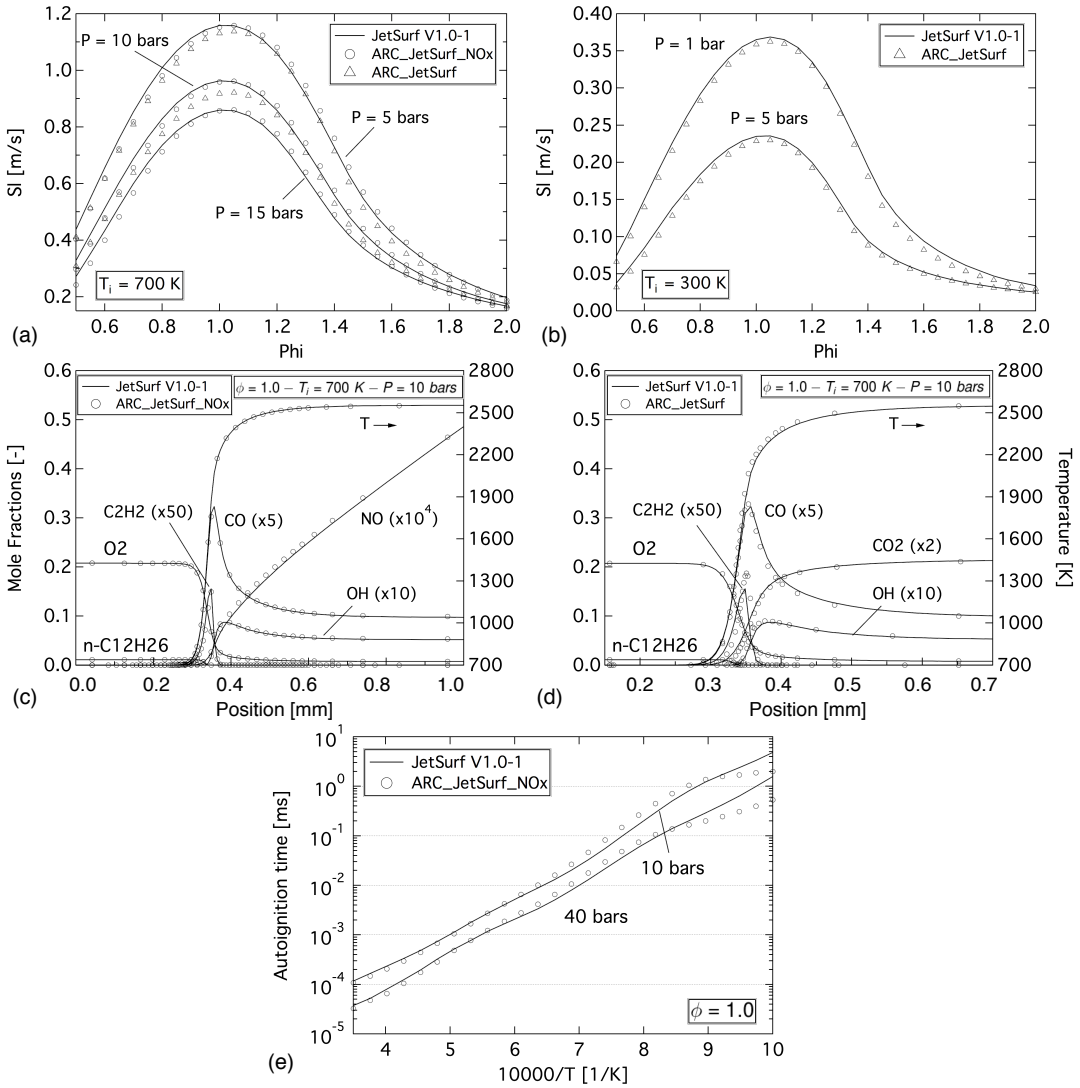

Fig. 16 Example of performances of the ARC_JetSurf and ARC_JetSurf_NOx on canonical UPF test cases: (a)-(b) laminar flame speed versus equivalence ratio for different pressure and initial temperature, (c)-(d) evolution of the major species and temperature across a canonical UPF for P = 10 bars, $T_i = 700$ K and $\phi = 1.0$. (d) Example of CVR cases results with the ARC_JetSurf_NOx. Comparisons are performed with the relevant detailed mechanism [86,85].

4.5 Jet A

4.6 HyChem model for the Jet A POSF10325

Very often, the surrogate formulation for a real fuel like aviation kerosene relies upon the selection of a few representative hydrocarbon components. Typically, from one to four components are retained, including *n*/*iso*/*cyclo*-alkanes and aromatics [11]. However, an alternative approach was recently proposed, based on experimental observations: the HyChem model [103,102]. The methodology relies on the assumption that any fuel, no matter its complexity, decompose into a handful of components, and that it is the distribution of these pyrolysis products in the reaction zone that impacts the subsequent radical buildup and heat release rate. The pyrolysis intermediates are dominated by hydrogen (H_2), methane (CH_4), ethylene (C_2H_4), propene (C_3H_6), *iso*-butene (i-C_4H_8), 1-butene (1-C_4H_8), benzene (C_6H_6) and toluene (C_7H_8). In that sense, the combustion process can be decomposed into a fuel pyrolysis step and a subsequent oxidation of the pyrolysis products. The kinetic model for a particular real fuel can thus be obtained by merging a fuel-specific pyrolysis model comprised of a few lumped reactions, yielding the composition of the primary pyrolysis products, and a detailed foundational fuel chemistry model (C_1-C_4 kinetic mechanism). The "fuel", in that case, is a mono-component lumped species. Its pyrolysis model is derived from shock-tube and flow-reactor experiments. The resulting HyChem model captures shock-tube ignition delay times and laminar flame speeds over a wide range of pressure, temperature and equivalence ratio. It also predicts the counterflow non-premixed flame extinction strain rates over a range of fuel dilution.

Molecular formula	Composition (mass fraction [%])					Mol. Weight [kg/mol]
	Aromatics	*iso*-Paraffins	*n*-Paraffins	Cycloparaffins	Alkenes	
$C_{11.4}H_{22.1}$	18.66	29.45	20.03	31.86	<0.001	156.0
H/C	Δh_c [MJ/kg]	DCN	T_{10} [K]	$T_{90} - T_{10}$ [K]	μ_l(300 K) [mPa s]	ρ_l(300 K) [kg/m^3]
1.91	43.1	48.3	450.0	67.8	1.37	794

Table 11 Properties of the Jet-A POSF10325

The specific HyChem model considered for the reduction is that of an average, commercial Jet A fuel (POSF10325), which was procured from the Shell Mobile refinery in June 2013 as a part of tests conducted by the National Jet Fuel Combustion Program. Its properties are summarized in Table 11.

4.7 Derivation of ARCs for the Jet A POSF10325

Based on the HyChem model, two ARCs for the oxidation of Jet A have been derived. They were both designed to target partially premixed applications under atmospheric conditions, and to properly account for the decomposition of the main pyrolysis products (C_2H_4, C_6H_6, C_2H_2). One of the ARCs, referred to as the ARC_HYCHEM_NOx, was supplemented with a reduced version of the Luche NO_x submechanism [59] to account for NO global and local production. Details about the derivation and validation range as well as the list of retained transported and QSS species are provided in Table 12. Figure 17 and 18 illustrate the performances of both ARCs on various canonical test cases, targeted and non-targeted by the derivation. In particular, note that the reduced mechanisms are still valid (provided that the detailed mechanism is still valid!) under relatively high operating pressures, more representative of current aero-engines design.

Fuel/Oxidant	Jet A (POSF10325)/Air	Jet A (POSF10325)/Air
Purpose	Partially premixed applications CO analysis	Partially premixed applications NO and CO analysis
Detailed mechanism	USC II [99] + pyrolysis steps [103,102]	USC II [99] + pyrolysis steps [103,102]
Number of transported species/reactions/QSS	27/268/12	29/518/17
Transported species	H H_2 O O_2 OH H_2O HO_2 H_2O_2 CH_3 CH_4 C_2H_2 C_2H_4 C_2H_6 C_3H_6 aC_3H_4 i-C_4H_8 C_5H_6 C_6H_6 $C_6H_5CH_3$ CO CO_2 CH_2O CH_2CO C_6H_5O $C_6H_4O_2$ N_2 POSF10325	H H_2 O O_2 OH H_2O HO_2 H_2O_2 CH_3 CH_4 C_2H_2 C_2H_4 C_2H_6 C_3H_6 i-C_4H_8 C_5H_6 C_6H_6 $C_6H_5CH_3$ CO CO_2 CH_2O CH_2CO C_6H_5O $C_6H_4O_2$ N_2 NO NO_2 HCN POSF10325
QSS species	CH_2 CH_2* C_2H_3 C_2H_5 aC_3H_5 C_6H_5 $C_6H_5CH_2$ HCO CH_3O HCCO CH_2CHO C_6H_5CHO	CH CH_2 CH_2* C_2H_3 C_2H_5 aC_3H_5 C_6H_5 HCO CH_3O HCCO CH_2CHO N NH CN H_2CN HNO NCO
Targeted canonical test cases	UPF: P = 1 bar T = 300 K ϕ = [0.8-1.3] AI: P = 1 bar T = [1300-1700] K ϕ = [0.8-1.3]	UPF: P = 1 bar T = 300 K ϕ = [0.8-1.3] AI: P = 1 bar T = [1300-1700] K ϕ = [0.8-1.3]
Targeted quantities	UPF: s_l, T_b, OH, CO, pyrolysis products AI: τ_{ig}, T, OH, CO	UPF: s_l, T_b, OH, CO, NO, pyrolysis products AI: τ_{ig}, T, OH, CO
Validation range (for the targeted quantities)	UPF: P = [1-10] bars T = [300] K ϕ = [0.5-1.5] AI: P = [1-40] bars T = [1000-3000] K ϕ = [0.5-1.5]	UPF: P = [1-10] bars T = [300] K ϕ = [0.5-1.5] AI: P = [1-40] bars T = [1000-3000] K ϕ = [0.5-1.5]
Refs (more validations)	[13,16]	[13,14]

Table 12 YARC derived ARCs for Jet A combustion

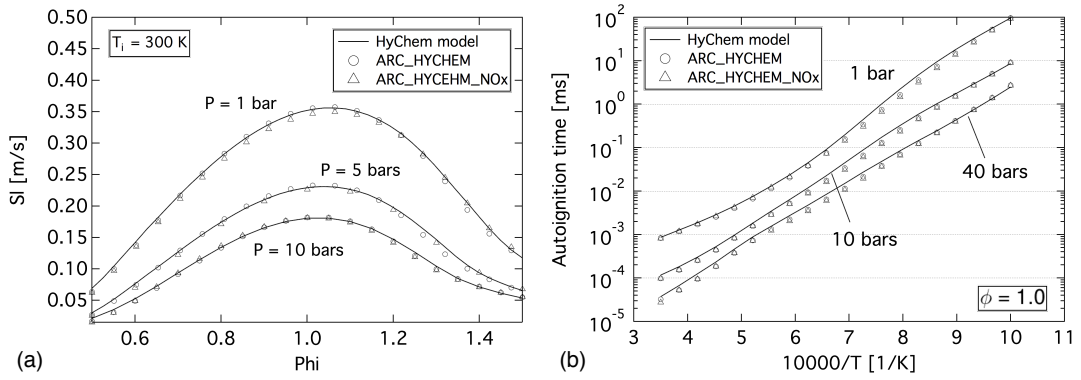

Fig. 17 Example of performances of the ARC_HYCHEM and ARC_HYCHEM_NOx on (a) canonical UPF test cases and (b) canonical CVR test cases. Comparisons are performed with the relevant detailed HYCHEM model [102,99].

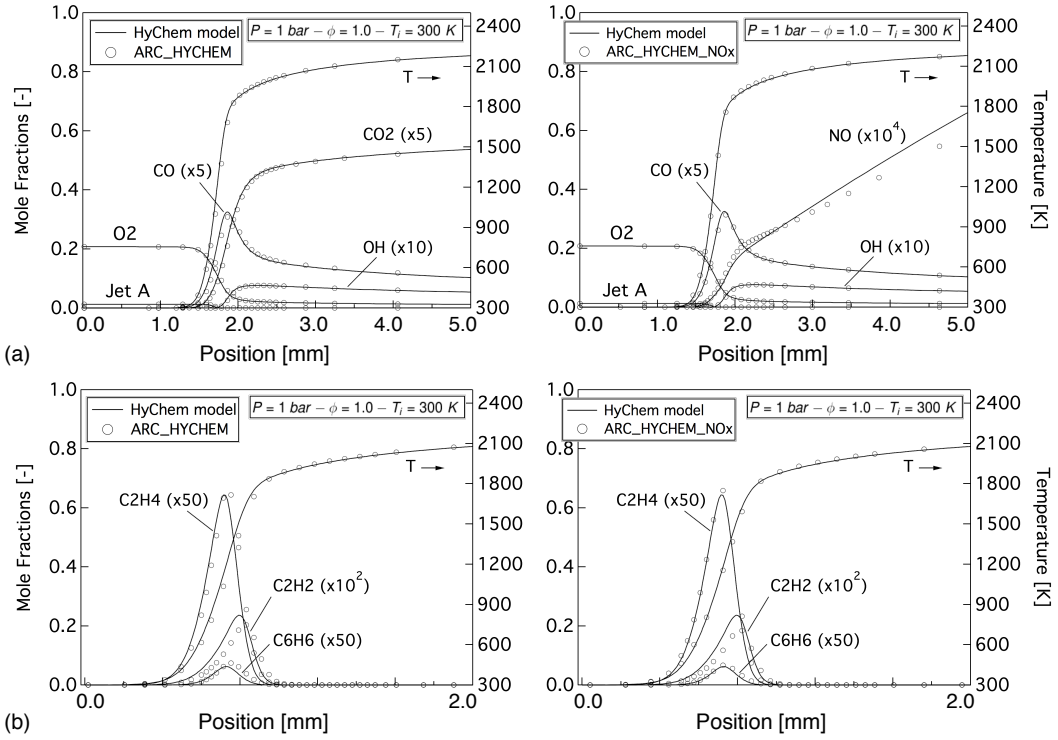

Fig. 18 Evolution of (a) major species and temperature and (b) major intermediates across canonical UPF for P = 1 bar, $T_i = 300$ K and $\phi = 1.0$, with both ARCs derived based on the HYCHEM model. Comparisons are performed with the relevant detailed HYCHEM model [102, 99].

5 ARC for LES of turbulent combustion: general trends

5.1 Size of ARCs

Figure 19 reports correlations between species and reactions contained in a collection of ARCs. Two ARCs for methane-air combustion and one ARC for ethylene-air oxidation reported in the literature [53] were added to those presented in this paper. Data from an in-house ARC for iso-octane combustion were also added, to bridge the gap between the small hydrocarbons and kerosene surrogates. Each circle represents one ARC. Red circles represent ARCs containing a NO_x sub-mechanism, blue circles represent ARCs with the prospect of soot modeling, and dark circles represent ARCs not targeting pollutants.

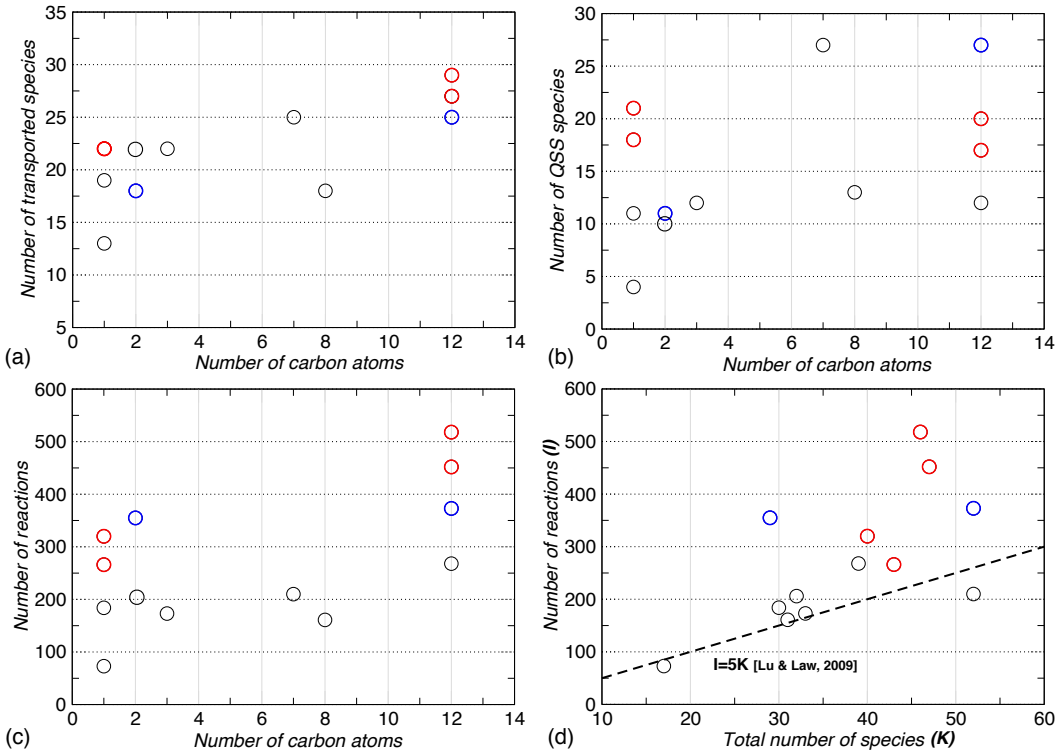

Fig. 19 Number of (a) transported species (b) QSS species (c) reactions versus number of carbon content in each hydrocarbon. (d) Number of reactions versus the total number of species contained (transported + QSS) in each ARC. The line reports the tendency observed by Lu & Law [57].

One interesting observation is that the number of reactions to consider (Fig. 19 (d)) seem to be greatly impacted by the decision to include the formation of pollutants. It is particularly true of NO, requiring to take into account many additional pathways involving azoted species. Of course, these additional reactions are associated with an additional set of species, that must also be accounted for in the ARC. However, as can be seen in Figs. 19 (a)&(b), the overcost of species is less pronounced than the overcost of reactions. This causes the correlation between species and reactions contained in ARCs retaining a NO_x sub-mechanism to stray from the theoretical line of [57], reported in Fig. 19 (d). This is an important observation, indicating that, at least in terms of number of species to transport, any hydrocarbon can be accommodated in CFD.

5.2 Species to consider

Another interesting observation from the analysis of each ARC, either reported in the literature or YARC-derived, is that there appears to be a "core" of 14 species systematically identified as necessary and thus, retained whatever the hydrocarbon. These are: H, H_2, O, O_2, OH, H_2O, HO_2,

H_2O_2, CH_3, CH_4, CO, CO_2, CH_2O and N_2. For hydrocarbons with a carbon content of 2 or more, this list is appended with C_2H_2, C_2H_4 and C_2H_6. Note that HO_2, H_2O_2 or CH_3 are sometimes identified as potential QSS species, due to their small associated timescales. Moreover, most of the time, the 6 following species are retained as QSS: CH_2, CH_2*, C_2H_3, C_2H_5, HCO and HCCO.

If NO is of interest, NO_2, N_2O and HCN are usually retained, to account for the various NO pathways. These species are added to the list of transported species. Additionally in this case, CH becomes necessary, being a key intermediate in many thermal pathways. It is usually put in QSS.

5.3 Stiffness of ARCs

One major drawback associated with the use of ARC in CFD is that the chemical timescales involved can span a large range. Radical species are consumed as soon as they are produced, while the formation of NO or soot spreads over a few seconds. ARCs are thus always associated with stiffness. However, in most cases and with a careful derivation, stiffness can be reduced to a minimum by limiting the transport of species with very short associated timescales.

To that end, it is of interest to identify these "absolutely necessary" species, that are seen to induce stiffness. From an investigation of the ARCs considered in this paper, it appears that:

- For a fuel carbon content below 3, H_2O_2 is usually the species with the smallest associated timescale.
- For a fuel carbon content above 8 (typical kerosene surrogates), the fuel is usually the species with the smallest associated timescale.
- For propane and *n*-heptane, just as for many fuel species of intermediate size, the consideration of very short-lived radicals (C-4/C-5) will generally be required, complexifying the reduction process and possibly resulting in relatively stiff mechanisms.

These considerations are illustrated in Fig. 20, showing the minimum chemical timescales involved in a laminar flame under atmospheric conditions, in a collection of ARCs. The timescale evaluation is based upon a Jacobian evaluation performed with perturbations.

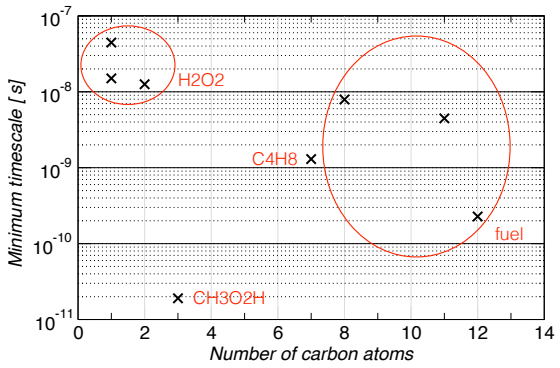

Fig. 20 Estimation of the minimum timescales involved in a canonical UPF case, under atmospheric conditions. The ARCs reported are YARC-derived ARCs, valid under atmospheric conditions.

6 Conclusions

In this paper, a multi-reduction automated tool, YARC, was employed to derive LES-compliant ARCs for various hydrocarbons and applications. The methodology is proven to be very efficient, enabling in particular to fully control stiffness and the maximum allowed error on targeted quantities. One major finding of this study is that any hydrocarbon, from the smallest, methane or ethylene, to the heavier multi-component aviation kerosenes can be directly accommodated in modern CFD applications, with the current available CPU resources.

The reported ARCs are made available to the community, and can be found online [7].

References

1. Alison, S.T., Turányi, T., Pilling, M.J.: Mathematical tools for the construction, investigation and reduction of combustion mechanisms. (Chap. 4). Comprehensive Chemical Kinetics **35**, 293 – 437 (1997). DOI http://dx.doi.org/10.1016/S0069-8040(97)80019-2. URL http://www.sciencedirect.com/science/article/pii/S0069804097800192
2. Avdić, A., Kuenne, G., di Mare, F., Janicka, J.: LES combustion modeling using the Eulerian stochastic field method coupled with tabulated chemistry. Combustion and Flame **175**, 201–219 (2017)
3. Baritaud, T., Poinsot, T., Baum, M.: Direct Numerical Simulation for turbulent reacting flows. Editions Technip (1996)
4. Bauerheim, M., Jaravel, T., Esclapez, L., Riber, E., Gicquel, L.Y.M., Cuenot, B., Cazalens, M., Bourgois, S., Rullaud, M.: Multiphase flow Large-Eddy Simulation study of the fuel split effects on combustion instabilities in an ultra-low-nox annular combustor. Journal of Engineering for Gas Turbines and Power **138**(6), 061,503 (2016)
5. Bowman, C.T., Frenklach, M., Gardiner, W.R., Smith, G.: The GRI-Mech 3.0 chemical kinetic mechanism. University of California: Berkeley, CA (1999)
6. Bowman, C.T., Hanson, R.K., Davidson, D.F., Jr, W.C.G., Lissianski, V., Smith, G.P., Golden, D.M., Frenklach, M., Goldenberg, M.: GRI-Mech 2.11. URL: http://www.me.berkeley.edu/gri-mech (1995)
7. CERFACS: YARC derived ARCs for combustion applications. http://www.cerfacs.fr/cantera (2017)
8. Charles, W.K., Mizobuchi, Y., Poinsot, T.J., Smith, P.J., Warnatz, J.: Computational combustion. Proceedings of the Combustion Institute **30**(1), 125–157 (2005)
9. Chen, J.: Development of reduced mechanisms for numerical modelling of turbulent combustion. In: Workshop on Numerical Aspects of Reduction in Chemical Kinetics, CERMICS-ENPC, Cite Descartes, Champus sur Marne, France. Reno, NV (1997)
10. Chen, J.H.: Petascale direct numerical simulation of turbulent combustion - fundamental insights towards predictive models. Proceedings of the Combustion Institute **33**(1), 99–123 (2011)
11. Edwards, T., Maurice, L.Q.: Surrogate mixtures to represent complex aviation and rocket fuels. Journal of propulsion and power **12**(2) (2001)
12. Esclapez, L., Ma, P.C., Mayhew, E., Rui, X., Stouffer, S., Lee, T., Wang, H., Ihme, M.: Fuel effects on lean blow-out in a realistic gas turbine combustor. Combustion and Flame **181**, 82–99 (2017)
13. Felden, A.: Development of Analytically Reduced Chemistries (ARC) and applications in Large Eddy Simulations (LES) of turbulent combustion. Phd thesis, CERFACS (2017)
14. Felden, A., Esclapez, L., Misdariis, A., Riber, A., Wang, H., Cuenot, B.: Including real fuel chemistry in Large-Eddy Simulations. 7th EUCASS Proceedings (2017)
15. Felden, A., Riber, E., Cuenot, B.: Impact of direct integration of Analytically Reduced Chemistry in LES of a sooting swirled non-premixed combustor. Submitted to Combustion and Flame pp. – (2017)
16. Felden, A., Riber, E., Cuenot, B., Esclapez, L., Ihme, M., Wang, H.: Including real fuel chemistry in LES of turbulent combustion. In: Proc. of the Summer Program, pp. –. Center for Turbulence Research, Stanford Univ. (2016)
17. Fiorina, B., Gicquel, O., Carpentier, S., Darabiha, N.: Validation of the FPI chemistry reduction method for diluted nonadiabatic premixed flames. Combustion science and technology **176**(5-6), 785–797 (2004)
18. Fiorina, B., Gicquel, O., Vervisch, L., Carpentier, S., Darabiha, N.: Approximating the chemical structure of partially premixed and diffusion counterflow flames using FPI flamelet tabulation. Combustion and flame **140**(3), 147–160 (2005)
19. Fiorina, B., Veynante, D., Candel, S.: Modeling combustion chemistry in Large-Eddy Simulation of turbulent flames. Flow, Turbulence and Combustion **94**, 3–42 (2015)
20. Franzelli, B., Fiorina, B., Darabiha, N.: A tabulated chemistry method for spray combustion. Proceedings of the Combustion Institute **34**(1), 1659–1666 (2013)
21. Franzelli, B., Riber, E., Sanjose, M., Poinsot, T.: A two-step chemical scheme for kerosene–air premixed flames. Combustion and Flame**157**, 1364–1373 (2010)
22. Franzelli, B., Vié, A., Boileau, M., Fiorina, B., Darabiha, N.: Large-Eddy Simulation of swirled spray flame using detailed and tabulated chemical descriptions. Flow, Turbulence and Combustion pp. 1–29 (2016)
23. Frouzakis, C.E., Boulouchos, K.: Analysis and reduction of the CH4-Air mechanism at lean conditions. Combustion Science and Technology**159**, 281–303 (2000)
24. Fureby, C.: A comparative study of flamelet and finite rate chemistry LES for a swirl stabilized flame. Journal of Engineering for Gas Turbines and Power **134**(4), 041,503 (2012)
25. Gallot-Lavallee, S., Jones, W.P.: Large-Eddy Simulation of spray auto-ignition under EGR conditions. Flow Turbulence and Combustion **96**, 513–534 (2016)
26. Gicquel, L.Y.M., Staffelbach, G., Poinsot, T.J.: Large-Eddy Simulations of gaseous flames in gas turbine combustion chambers. Progress in Energy and Combustion Science**38**, 782–817 (2012)
27. Gicquel, O., Darabiha, N., Thévenin, D.: Laminar premixed hydrogen/air counterflow flame simulations using flame prolongation of ildm with differential diffusion. Proceedings of the Combustion Institute **28**, 1901–1908 (2000)
28. Giusti, A., Mastorakos, E.: Detailed chemistry LES/CMC simulation of a swirling ethanol spray flame approaching blow-off. Proceedings of the Combustion Institute (2016)
29. Goodwin, D.G., Moffat, H.K., Speth, R.L.: Cantera: An object-oriented software toolkit for chemical kinetics, thermodynamics, and transport processes. http://www.cantera.org (2014). Version 2.1.2
30. Goussis, D.A., Lam, S.H.: A study of homogeneous methanol oxidation kinetics using CSP. Symposium (International) on Combustion **24**(1), 113–120 (1992)
31. Goussis, D.A., Mass, U.: Model reduction for combustion chemistry. In: T. Echekki, E. Mastorakos Turbulent Combustion Modeling, Fluid Mechanics and Its Applications **95**, 193–220 (2011)

32. Griffiths, J.F.: Reduced kinetic models and their application to practical combustion systems. Progress in Energy and Combustion Science**21**, 25–107 (1995)
33. Hamby, D.M.: A review of techniques for parameter sensitivity analysis of environmental models. Environmental Monitoring and Assessment **32**, 135–154 (1994)
34. Haworth, D.C., J., T., Poinsot: Numerical simulations of lewis number effects in turbulent premixed flames. Journal of Fluid Mechanics **244**, 405–436 (1992)
35. Huang, H., Fairweather, M., Griffiths, J.F., Tomlin, A.S., Brad, R.B.: A systematic lumping approach for the reduction of comprehensive kinetic models. Proceedings of the Combustion Institute **30**, 1309–1316 (2005)
36. Ihme, M., Pitsch, H.: Modeling of radiation and nitric oxide formation in turbulent nonpremixed flames using a flamelet/progress variable formulation. Physics of Fluids **20**(5), 055,110 (2008)
37. Jaouen, N.: An automated approach to derive and optimise reduced chemical mechanisms for turbulent combustion. Phd thesis, CORIA (2017)
38. Jaouen, N., Vervisch, L., Domingo, P., Ribert, G.: Automatic reduction and optimisation of chemistry for turbulent combustion modelling: Impact of the canonical problem. Combustion and Flame (2016)
39. Jaravel, T.: Prediction of pollutants in gas turbines using Large-Eddy Simulation. Phd thesis, CERFACS (2016)
40. Jaravel, T., Riber, E., Cuenot, B., Bulat, G.: Large-Eddy Simulation of an industrial gas turbine combustor using reduced chemistry with accurate pollutant prediction. Proceedings of the Combustion Institute (2016)
41. Jerzembeck, S., Peters, N., Pepiot-Desjardins, P., Pitsch, H.: Laminar burning velocities at high pressure for primary reference fuels and gasoline: Experimental and numerical investigation. Combustion and Flame **156**(2), 292–301 (2009)
42. Jones, W.P., Lindstedt, R.P.: Global reaction schemes for hydrocarbon combustion. Combustion and flame **73**(3), 233–249 (1988)
43. Jones, W.P., Marquis, A.J., Prasad, V.N.: LES of a turbulent premixed swirl burner using the eulerian stochastic field method. Combustion and Flame **159**(10), 3079–3095 (2012)
44. Jones, W.P., Tyliszczack, A.: Large-Eddy Simulation of spark ignition in a gas turbine combustor. Flow, Turbulence and Combustion**85**(3-4), 711–734 (2010)
45. Kee, R.J., Rupley, F.M., Miller, J.A.: Chemkin-II: A Fortran chemical kinetics package for the analysis of gas-phase chemical kinetics. Tech. Rep. SAND-89-8009, Sandia National Labs., Livermore, CA (USA) (1989)
46. Knudsen, E., Pitsch, H.: A general flamelet transformation useful for distinguishing between premixed and non-premixed modes of combustion. Combustion and flame **156**(3), 678–696 (2009)
47. Laboratory, L.L.N.: Primary Reference Fuels (PRF): iso-octane / n-heptane mixtures. https://combustion.llnl.gov/archived-mechanisms/surrogates/prf-isooctane-n-heptane-mixture (2004)
48. Lam, H.S., Goussis, D.A.: The CSP method for simplifying kinetics. International Journal of Chemical Kinetics **26**, 461–486 (1994)
49. Lecocq, G., Poitou, D., Hernández, I., Duchaine, F., Riber, E., Cuenot, B.: A methodology for soot prediction including thermal radiation in complex industrial burners. Flow, Turbulence and Combustion **92**, 947–970 (2014)
50. Lefebvre, A.H.: Gas Turbine Combustion, second edn. Taylor & Francis (1998)
51. Liu, S., Hewson, J.C., Chen, J.H., Pitsch, H.: Effects of strain rate on high-pressure nonpremixed n-heptane autoignition in counterflow. Combustion and flame **137**(3), 320–339 (2004)
52. Lovas, T., Nilsson, D., Mauss, F.: Automatic reduction procedure for chemical mechanisms applied to premixed methane/air flames. Proceedings of the Combustion Institute **28**, 1809–1815 (2000)
53. Lu, T.: Reduced mechanisms for combustion applications. http://www.engr.uconn.edu/ tlu/mechs/mechs.htm (2008)
54. Lu, T., Law, C.K.: A directed relation graph method for mechanism reduction. Proceedings of the Combustion Institute **30**, 1333–1341 (2005)
55. Lu, T., Law, C.K.: A criterion based on computational singular perturbation for the identification of quasi steady state species: A reduced mechanism for methane oxidation with no chemistry. Combustion and Flame **154**(4), 761–774 (2008)
56. Lu, T., Law, C.K.: Strategies for mechanism reduction for large hydrocarbons: n-heptane. Combustion and flame **154**(1), 153–163 (2008)
57. Lu, T., Law, C.K.: Toward accommodating realistic fuel chemistry in large-scale computations. Progress in Energy and Combustion Science **35**(2), 192–215 (2009)
58. Lu, T., Plomer, M., Luo, Z., Sarathy, S., Pitz, W., Som, S., Longman, D.: Directed relation graph with expert knowledge for skeletal mechanism reduction. In: 7th US National Combustion Meeting (2011)
59. Luche, J.: Obtention de modeles cinétiques réduits de combustion. application à un mécanisme du kérosène. Phd thesis, Université d'Orléans (2003)
60. Maas, U., Pope, S.B.: Simplifying chemical kinetics: intrinsic low-dimensional manifolds in composition space. Combustion and flame **88**(3), 239–264 (1992)
61. Massias, A., Diamantis, D., Mastorakos, E., Goussis, D.A.: An algorithm for the construction of global reduced mechanisms with CSP data. Combustion and Flame **117**, 685–708 (1999)
62. Mouriaux, S.: Large Eddy simulation of the turbulent spark ignition and of the flame propagation in spark ignition engines. Phd thesis, EM2C (2016)
63. Mueller, M.E., Pitsch, H.: LES model for sooting turbulent nonpremixed flames. Combustion and Flame **159**(6), 2166–2180 (2012)
64. Mueller, M.E., Pitsch, H.: Large-Eddy Simulation of soot evolution in an aircraft combustor. Physics of Fluids **25**(11), 110,812 (2013)
65. Narayanaswamy, K., Blanquart, G., Pitsch, H.: A consistent chemical mechanism for oxidation of substituted aromatic species. Combustion and Flame **157**, 1879–1898 (2010)
66. Navarro-Martinez, S., Kronenburg, A.: LES/CMC simulations of a turbulent bluff-body flame. Proceedings of the Combustion Institute **31**(2), 1721–1728 (2007)

67. Nguyen, P.D., Vervisch, L., Subramanian, V., Domingo, P.: Multidimensional flamelet-generated manifolds for partially premixed combustion. Combustion and Flame **157**(1), 43–61 (2010)
68. Norris, A.T., Pope, S.B.: Modeling of extinction in turbulent diffusion flames by the velocity-dissipation-composition PDF method. Combustion and Flame **100**(1-2), 211–220 (1995)
69. Oijen, J.A.V., Lammers, F.A., Goey, L.P.H.D.: Modeling of complex premixed burner systems by using flamelet-generated manifolds. Combustion and Flame **127**(3), 2124–2134 (2001)
70. Pepiot, P.: Automatic strategies to model transportation fuel surrogates. Phd thesis, Stanford University (2008)
71. Pepiot, P., Pitsch, H.: A chemical lumping method for the reduction of large chemical kinetic mechanisms. Combustion Theory and Modelling **12:6**, 1089 – 1108 (2008)
72. Pepiot-Desjardins, P., Pitsch, H.: An efficient error propagation based reduction method for large chemical kinetic mechanisms. Combustion and Flame **154**, 67–81 (2008)
73. Peters, N., Rogg, B.: Reduced kinetic mechanisms for applications in combustion systems. Lecture Notes in Physics, Berlin Springer Verlag **15** (1993)
74. Philip, M., Boileau, M., Vicquelin, R., Riber, E., Schmitt, T., Cuenot, B., Durox, D., Candel, S.: Large-Eddy Simulations of the ignition sequence of an annular multiple-injector combustor. Proceedings of the Combustion Institute **35**(3), 3159–3166 (2015)
75. Pierce, C.D., Moin, P.: Progress-variable approach for Large-Eddy Simulation of non-premixed turbulent combustion. Journal of Fluid Mechanics **504**, 73–97 (2004)
76. Pitsch, H.: FlameMaster v3.1. A C++ computer program for 0D combustion and 1D laminar fame calculations (1988)
77. Poinsot, T., Veynante, D.: Theoretical and numerical combustion, second edition. R.T. Edwards (2005). Out
78. Ranzi, E., Frassoldati, A., Grana, R., Cuoci, A., Faravelli, T., Kelley, A.P., Law, C.K.: Hierarchical and comparative kinetic modeling of laminar flame speeds of hydrocarbon and oxygenated fuels. Progress in Energy and Combustion Science **38**(4), 468–501 (2012)
79. Revel, J., Boettner, J.C., Cathonnet, M., Bachman, J.S.: Derivation of a global chemical kinetic mechanism for methane ignition and combustion. Journal de chimie physique **91**(4), 365–382 (1994)
80. Rochette, B., Collin-Bastiani, F., Gicquel, L., Vermorel, O., Poinsot, T., Veynante, D.: Influence of chemical schemes, numerical method and dynamic turbulent combustion modeling on LES of premixed turbulent flames. In preparation pp. – (2017)
81. Rogg, B.: A computer program for the simulation of one-dimensional chemically reacting flows. Tech. Rep. CUED/A-THERMO/TR39, Cambridge University (1991)
82. Sankaran, R., Hawkes, E., Chen, J., Lu, T., Law, C.: Structure of a spatially developing turbulent lean methane–air bunsen flame. Proceedings of the Combustion Institute **31**(1), 1291–1298 (2007)
83. Schulz, O., Jaravel, T., Poinsot, T., Cuenot, B., Noiray, N.: A criterion to distinguish autoignition and propagation applied to a lifted methane–air jet flame. Proceedings of the Combustion Institute **36**(2), 1637–1644 (2017)
84. Selle, L., Lartigue, G., Poinsot, T., Koch, R., Schildmacher, K.U., Krebs, W., Prade, B., Kaufmann, P., Veynante, D.: Compressible Large-Eddy Simulation of turbulent combustion in complex geometry on unstructured meshes. Combustion and Flame**137**, 489–505 (2004)
85. Sirjean, B., Dames, E., Sheen, D.A., Wang, H.: A simplified version of the high-temperature chemical kinetic model of n-alkane oxidation, JetSurF version 1.0. https://web.stanford.edu/group/haiwanglab/JetSurF/JetSurF1.0/Reduced Model/JetSurF1.0-l.html (2009)
86. Sirjean, B., Dames, E., Sheen, D.A., You, X.Q., Sung, C., Holle, A.T., Egolfopoulos, F.N., Wang, H., Vasu, S.S., Davidson, D.F., Hanson, R.K., Pitsch, H., Bowman, C.T., Kelley, A., Law, C.K., Tsang, W., Cernansky, N.P., Miller, D.L., Violi, A., Lindstedt, R.P.: A high-temperature chemical kinetic model of n-alkane oxidation, JetSurF version 1.0. http://web.stanford.edu/group/haiwanglab/JetSurF/JetSurF1.0/index.html (2009)
87. Smooke, M.D., Giovangigli, V.: Reduced kinetic mechanisms and asymptotic approximations for methane–air flames. Lecture Notes in Physics, Springer-Verlag **15** (1991)
88. Tomlin, A.S., Pilling, M.J., Turányi, T.: Mechanism reduction for the oscillatory oxidation of hydrogen: Sensitivity and quasi-steady-state analyses. Combustion and Flame **91**, lO7–130 (1992)
89. Turányi, T.: List of publications including reduced mechanisms for combustion applications. http://garfield.chem.elte.hu/Turanyi/ttpub.html (1981)
90. Turányi, T.: Reduction of large reaction mechanisms. New Journal of Chemistry **14**, 795–803 (1990)
91. Turányi, T.: Sensitivity analysis of complex kinetic systems: Tools and applications. Journal of Mathematical Chemistry **5**, 203–248 (1990)
92. Turányi, T., Tóth, J.: Comments to an article of Frank-Kamenetskii on the Quasi-Steady-State Approximation. Acta Chimica Hungarica **129**, 903–903 (1992)
93. Turányi, T., Zalotai, L., Dobe, S., Berces, T.: Applications of sensitivity analysis to combustion chemistry. Reliability Engineering and System Safety **57**, 41–48 (1997)
94. Vadja, S., Valkó, P., Turányi, T.: Principal component analysis of kinetic models. International Journal of Chemical Kinetics **17**, 55–81 (1985)
95. Veynante, D., Poinsot, T.: Reynolds averaged and Large-Eddy Simulation modeling for turbulent combustion. In: J.F.O. Metais (ed.) New tools in turbulence modelling. Lecture 5, pp. 105–135. Les editions de Physique, Springer (1997)
96. Vreman, A.W., Albrecht, B.A., Oijen, J.V., p. H. De Goey, L., Bastiaans, R.J.M.: Premixed and non-premixed generated manifolds in Large-Eddy Simulation of Sandia flame D and F. Combustion and Flame **153**(3), 394–416 (2008)
97. Wang, H., Frenklach, M.: A detailed kinetic modeling study of aromatics formation in laminar premixed acetylene and ethylene flames. Combustion and flame **110**(1), 173–221 (1997)
98. Wang, H., Laskin, A., Djurisic, Z.M., Law, C.K., Davis, S.G., Zhu, D.L.: A comprehensive mechanism of c2hx and c3hx fuel combustion. Fall Technical Meeting of the Eastern States Section of the Combustion Institute, Raleigh, NC, Oct pp. 129–132 (1999)

99. Wang, H., You, X., Joshi, A.V., Davis, S.G., Laskin, A., Egolfopoulos, F., Law, C.K.: USC Mech Version II. High-Temperature Combustion Reaction Model of H2/CO/C1-C4 Compounds. http://ignis.usc.edu/USC_Mech_II.htm (2007)
100. Warnatz, J., Maas, U., Dibble, R.: Combustion: physical and chemical fundamentals, modeling and simulation, experiments, pollutant formation (1995)
101. Westbrook, C.K., Dryer, F.L.: Simplified reaction mechanisms for the oxidation of hydrocarbon fuels in flames. Combustion Science and Technology **27**, 31–43 (1981)
102. Xu, R., Chen, D., Wang, K., Tao, Y., Shao, J.K., Parise, T., Zhu, Y., Wang, S., Zhao, R., Lee, D.J., Egolfopoulos, F.N., Davidson, D.F., Hanson, R.K., Bowman, C.T., Wang, H.: Hychem model: Application to petroleum-derived jet fuels. 10th US National Meeting on Combustion, College Park, MD (2017)
103. Xu, R., Wang, H., Davidson, D.F., Hanson, R.K., Bowman, C.T., Egolfopoulos, F.N.: Evidence supporting a simplified approach to modeling high-temperature combustion chemistry. 10th US National Meeting on Combustion, College Park, MD (2017)
104. You, X., Egolfopoulos, F.N., Wang, H.: Detailed and simplified kinetic models of n-dodecane oxidation: The role of fuel cracking in aliphatic hydrocarbon combustion. Proceedings of the Combustion Institute **32**(1), 403–410 (2009)
105. Zambon, A.C., Chelliah, H.K.: Explicit reduced reaction models for ignition, flame propagation, and extinction of C2H4/CH4/H2 and air systems. Combustion and flame **150**(1), 71–91 (2007)